Spacing of Aerators for Spillways

Development of a 2-D numerical model

R W P May
M Escarameia

Report SR 311
May 1992

HR Wallingford

Registered Office: HR Wallingford Ltd, Howbery Park, Wallingford, Oxfordshire OX10 8BA, UK
Telephone: 0491 35381 International + 44 491 35381 Telex: 848552 HRSWAL G.
Facsimile: 0491 32233 International + 44 491 32233 Registered in England No. 1622174

Contract

This report describes work partly funded by the Department of the Environment (DoE) under Research Contract PECD 7/6/231 for which the nominated officers were Mr P Woodhead for DoE and Dr W R White for HR Wallingford. The HR job number was RQS 0023. It is published on behalf of the Department of the Environment, but any opinions expressed in this report are not necessarily those of the funding Department. The work was carried out by M Escarameia and R W P May who also managed the project.

This report forms the contract completion report for the study.

Prepared by ....RWP. May.... Manuela Escarameia

Checked by ....RWP. May.... ....

Approved by ....RWP. May....

Date....29-5-92....

Summary

Spacing of aerators for spillways
Development of a 2-D numerical model

R W P May
M Escarameia

Report SR 311
May 1992

This report describes the development and testing of a numerical diffusion/ advection model (ADAM) to calculate air concentration profiles downstream of spillway aerators. The study was funded by the Construction Directorate of the Department of the Environment and by HR Wallingford.

This numerical model is the latest of a series of studies on the performance of aerators carried out at HR Wallingford. The first stage included a comprehensive literature review on cavitation and aeration in spillways, which was followed by an experimental study of air demand in ramp aerators. A numerical model was also produced to assist in the choice and design of alternative layouts of spillways and aerators.

Program ADAM was developed to model the rate at which the air decreases with distance along the spillway downstream of an aerator. This rate determines where the next aerator should be located in order to maintain protection against cavitation damage. ADAM is a 2-D model written in FORTRAN 77 which uses an explicit finite-difference scheme to model the changes in air concentration. These depend on four competing effects : advection of the air bubbles by the flow of water; upward movement of the bubbles (buoyancy effect); diffusion due to turbulence in the water; and downward entrainment of air through the free surface. The governing diffusion/ advection equation was adapted to cover the particular case of two-phase flows in which the proportions of the two phases are similar in magnitude. The equation is first solved for a "virtual" non-aerated flow and the results then transformed to apply to the equivalent aerated flow.

ADAM was calibrated with experimental data for self-aeration and tested against data from two model studies of spillway aerators and one field study of self-aeration in a prototype spillway. Results from ADAM are applicable in the lower region of an aerated flow where the air/water mixture consists mainly of air bubbles and water; for the upper region, formed by water droplets in air, no suitable governing equations have yet been developed.

The development of the present program has highlighted a current lack of information about the following factors: typical air bubble sizes in high-velocity flows; relationship between bubble size and effective rise velocity in turbulent flows with high air concentrations; diffusion coefficients for aerated flows; effect of flow curvature in reattachment zones downstream of aerators; and initial air concentration profiles produced by aerators.

While existing 1-D models can only estimate depth-averaged air concentrations, the program described in this report is able to predict the distribution with depth and therefore gives values of air concentration along the channel bed. This information is essential for identifying the location and spacing of aerators needed to prevent cavitation damage.

For further information please contact the Hydrodynamics Group of the Research Department.

List of Symbols

A	Cross-sectional area of bubble
a	Resultant of g and centripetal acceleration
B	Net buoyancy force
C	Concentration
C_d	Drag coefficient
C_L	Limiting concentration
$\bar{C}$	Mean concentration
$\bar{C}_e$	Equilibrium value of the mean concentration
c	Coefficient in Equation (37)
D	Diffusion coefficient
D_{max}	Maximum value of the diffusion coefficient
d	Equivalent diameter of air bubbles
E	Property of flow
F	Drag force
F_x	Flux of air in the x direction
F_y	Flux of air in the y direction (aerated flow)
F_z	Flux of air in the z direction (equivalent non-aerated flow)
G	Coefficient in Equation (7)
g	Acceleration due to gravity
h	Total flow depth
J	Number of steps in the z direction
k	von Karman constant
k_s	Roughness height
N	Number of bubbles per unit volume of water
P	Pressure
q	Unit discharge of water
q_a	Unit discharge of air
R	Radius of vertical curvature of the spillway
R_e	Reynolds number of air bubbles ($= \frac{Wd}{\nu}$)
t	Time
U	Mean flow velocity
u	Component of velocity in the x direction
u_*	Shear velocity
V	Volume of air bubble
V_{en}	Entrainment velocity
$\dot{V}$	Net rate of inflow of air per unit area of free surface
v	Component of velocity in the y direction
W	Rise velocity of air bubbles
W_e	Equivalent rise velocity of air bubbles
W_N	Component of W_e normal to the channel
w	Fall velocity
x	Distance along the channel

List of Symbols *continued*

Y	Non-dimensional height above the bed ($= y/y_{90}$)
y	Level above the bed for aerated flow
y_L	Limiting level
y_t	Transition level
y_{90}	Level at which the air concentration is 90%
z	Height above the bed for non-aerated flow
α	Coefficient in Equation (9)
β	Air/water ratio (volumetric)
Δx	Longitudinal step
Δy	Step normal to the channel for aerated flow
Δz	Step normal to the channel for non-aerated flow
ε	Eddy viscosity
ν	Kinematic viscosity of water
ρ	Density of water
ρ_a	Density of air
θ	Channel slope
ϕ	Entrainment function
Ω	Potential function for body force

Contents

Contents continued

1 Introduction

Aerators are used to prevent damage by cavitation in spillways and tunnels of high-head dams. Cavities are formed in water if the local pressure head falls to about 10m below atmospheric pressure. Such pressures can be produced in chute spillways by localised flow separation at joints and channel irregularities if the velocity of the water typically exceeds 25m/s to 30m/s ; velocities of this order are likely to occur when the head below reservoir level is more than 40m to 50m. Serious damage to the perimeter of a concrete channel can be caused by the violent collapse of cavities. However, it has been found that sufficient air in the water provides a cushioning effect that is able to prevent damage occurring. If turbulence at the free surface does not entrain enough air downwards into the flow, aerators consisting of ramps and/or offsets in the channel can be used to draw in air naturally at the boundaries where it is most needed.

The first installations of aerators were made in the 1960's as remedial measures to spillway tunnels that had been damaged by cavitation ; early examples were Grand Coulee Dam (Colgate & Elder, 1961) and Yellowtail Dam (Borden et al, 1971), both in the USA. The first use of aerators on a chute spillway is believed to have been in Russia at Bratsk Dam (Semenkov & Lentjaev, 1973). However, until serious cavitation damage occurred to the Karun Dam in Iran (World Water, 1979), it was generally believed that the substantial thickness of the boundary layer on a spillway chute was sufficient to prevent the occurrence of cavitation. Following this experience, aerators were constructed as part of the Foz do Areia spillway in Brazil (Pinto et al, 1982) and were operated successfully at unit discharges up to 117m^3/s per metre width. Since then, aerators have tended to become standard features on new high-head spillways that are considered to be at risk from possible cavitation damage.

Although some prototype data are now available on the performance of spillway aerators (Pinto, 1991), most of the information and understanding has been obtained from laboratory studies where conditions can be controlled and studied in detail. As part of this research effort, HR Wallingford has carried out a series of studies funded by the Construction Directorate of the Department of the Environment (DoE). A comprehensive review of the literature on cavitation and aeration was produced in the first stage (May, 1987). A high-velocity flume was then constructed and an experimental study carried out to identify the factors affecting the air demand of ramp aerators (May & Deamer, 1989 and May, Brown & Willoughby, 1991). A numerical model called CASCADE was also produced that integrated an existing spillway-flow program with methods for predicting the performance of aeration systems (see the last-mentioned reference). This model provides a design tool that can be used to assess quickly and cheaply alternative layouts of spillways and aerators.

Although some important aspects of aerator performance require further study (due to the complex nature of the entrainment process), a reasonable foundation of information and experience is now established. However, relatively little is known about the behaviour of entrained air downstream of aerators. This question is important because the rate at which the air concentration decreases with distance along a spillway determines where the next aerator should be located in order to maintain protection against cavitation damage. Changes in air concentration depend upon four competing effects : advection (or transport) of the air bubbles by the flowing water ; upward movement depending on the size and buoyancy of the bubbles ; diffusion due to turbulence in the water ; and continued downward entrainment of air through the free surface. Studies of this problem carried out in physical models of spillways are subject to significant scale effects so the results cannot be reliably extrapolated to prototype situations. As a result, spacings of aerators tend at present to be estimated using simple rules-of-thumb that are based on very limited information.

This report describes the development and testing of a numerical diffusion/advection model called ADAM for simulating changes in air concentration downstream of aerators. A numerical approach was selected for two reasons. Firstly, the governing diffusion/advection equations have been used for a variety of problems (eg transport of suspended sediment), and suitable numerical methods therefore already exist for their solution. Secondly, the approach offers a means of overcoming the scale effects associated with the results of laboratory tests : the model can first be checked using values of the parameters appropriate to the laboratory data and then re-run with revised values suitable for conditions in the prototype. The numerical model was designed so that it could interface with the previously-developed CASCADE model, which determines flow conditions and cavitation risk along chute spillways and assists in the design of appropriate aeration systems.

Chapter 2 of this report reviews existing information relevant to the spacing of spillway aerators. Chapter 3 describes the derivation of the diffusion/ advection equation for the case of two-phase flow and its application to spillway problems. Chapter 4 describes the numerical model, including the finite-difference scheme and various alternative versions that were tested. Chapter 5 compares results from the model with available data from laboratory and prototype studies, and Chapter 6 identifies what further information and developments are needed to improve estimates of aerator spacing.

The funding for this study was provided by the Construction Directorate of DoE and by HR. The work was carried out between July 1991 and March 1992.

2 Existing information

2.1 Characteristics of aerated flows

An aerator normally works by causing flow to separate from the invert of a channel and form a large air cavity (as distinct from the small cavitation bubbles which are usually filled with water vapour). As the water passes over the cavity, air is entrained through the lower surface of the flow by the effects of turbulence and drag. It has also been found that strong entrainment can occur through the free surface due to the sudden pressure changes and turbulence which the aerator induces within the flow. Most aerators are designed so that air can be drawn into the cavity naturally without the use of fans ; this requires the pressure in the cavity to be below atmospheric. If the aerator does not cause a strong enough vertical curvature of the flow to overcome the hydrostatic head and produce a sub-atmospheric pressure, the cavity will collapse and fill with water.

Downstream of an aerator, the water flow reattaches to the invert of the channel and causes a rapid rise in pressure to a value above the hydrostatic pressure. This increase and the associated curvature of the streamlines produce a redistribution of the entrained air within the flow. Beyond this point, the flow becomes more uniform again with hydrostatic pressure and streamlines approximately parallel to the invert (on a time-mean basis). The longitudinal change in the amount of air in the flow and its distribution with depth then depend on the following factors:

1 Advection of the air bubbles along the channel by the high-velocity flow. Since the inertia of the air relative to the water is very small (about 1:820), the longitudinal velocity of the bubbles can be assumed to be effectively equal to that of the water.

2 Buoyancy of the air bubbles causing them to move upwards through the flow. It is normal to assume that, for a given bubble size and spillway curvature, the rise velocity is constant ; this corresponds to the buoyancy and drag forces being constant and in equilibrium due to the negligible inertia of the air bubbles in water. This assumption is clearly a fiction given the complex behaviour of turbulent two-phase mixtures so it is best to consider the rise velocity as an effective value that accounts for the overall observed behaviour.

3 Diffusion due to turbulence in the water causing a net transport of air from regions of higher to lower concentration. Values of the turbulent diffusion coefficient for single phase fluids are still the subject of continuing research. Very much less is known about values for two-phase mixtures (such as air and water), particularly when turbulence is generated by external features such as aerators.

4 Self-aeration at the free surface causing new air to be drawn down into the flow. Far enough along the channel, an equilibrium distribution of air will be attained when the net rate of loss of air through the free surface due to buoyancy and diffusion equals the rate of inflow due to self-aeration.

2.2 Self-aeration

Information about the general characteristics of the diffusion/advection process is provided by measurements of self-aerated flows. Although the entrainment mechanism at the free surface is somewhat different from that at an aerator, the distribution of air within the flow is governed by similar factors. The classic experiments on self-aeration were carried out by Straub & Anderson (1958), with further detailed studies being done by Gangadhariah et al (1970) ; useful summaries of the two sets of results are provided respectively by Henderson (1966) and Rao & Kobus (undated). These studies showed that a self-aerated flow can be divided into two regions:

1 lower region (or wall turbulent zone) consisting of air bubbles in water;
2 upper region (or free turbulent zone) consisting of water droplets in air.

It was found that air concentration profiles in the lower region fitted equations obtained by considering the balance between turbulent diffusion and the rise velocity of the bubbles. The concentration profiles in the upper region did not fit these equations but instead were found to have the shape of a Gaussian probability distribution ; this is consistent with the upper region containing water droplets that are projected randomly upwards from the lower region by turbulence. The transition level y_t between the two regions (and the corresponding sets of equations) was defined by Straub & Anderson as the point where the gradient of the concentration profile normal to the channel (dC/dy) was a maximum ; Gangadhariah et al defined the transition level as the point where the velocity profile normal to the channel was found to have a maximum (dU/dy = 0).

According to the results of Straub & Anderson, the upper droplet region only comes into existence when the mean concentration $\bar{C}$ of the flow exceeds about 25% ; its thickness then increases rapidly as the amount of self-aeration increases.

Gangadhariah et al further divided the wall turbulent zone into an inner and an outer layer. The air concentration profile within the inner layer (adjacent to the wall) was shown to be consistent with a turbulent diffusion coefficient that increased linearly with distance from the wall ; similarly the profile in the outer layer was consistent with a constant value of the diffusion coefficient. Results indicated that the inner layer of the wall turbulent zone only existed if the air concentration at the transition level y_t was less than about 20%. The variation of the diffusion coefficient with level is relevant to the performance of the numerical model described in this report, and is discussed again in Chapter 4.

An important conclusion from these studies on self-aeration is that a suitable diffusion/advection model should be capable of describing air concentration distributions within the lower region containing air bubbles in water.

However, the model is unlikely to be applicable in the upper region where differing governing equations apply ; here the flux of air is not caused by turbulent diffusion within the water but by drag forces exerted by rising and falling water droplets.

One-dimensional numerical models of the self-aeration process were developed by Ackers & Priestley (1985) and Wood (1985) for predicting changes in mean air concentration along a spillway. Both models are similar in concept and compute the flow profile down a spillway and the development of the boundary layer ; the spillway can have vertical curvature but cross waves due to horizontal curvature are not taken into account. In the Ackers & Priestley model self-aeration is assumed to start when the boundary layer reaches the surface ; Wood assumed that it starts somewhat earlier due to the break-through of turbulence when the flow depth is equal to 1.2 times the boundary-layer thickness. Both models simulate the self-aeration process by considering the balance of air fluxes into a control volume bounded by the channel invert and the free surface. Ackers & Priestley used the continuity relation:

$$\frac{d}{dx}[\bar{C}(1-\bar{C})] = \frac{\dot{V}}{q} \qquad (1)$$

where $\dot{V}$ is the net rate of inflow of air per unit area of free surface and q is the unit discharge of the water. The inflow rate was represented by the conceptual equation:

$$\dot{V} = V_{en} - \bar{C}\, W \cos\theta \qquad (2)$$

where V_{en} is the average velocity at which air is entrained downwards at the free surface and W is the rise velocity of the air bubbles ; the second term on the right-hand side therefore represents the rate at which air is lost from the flow due to buoyancy effects. When an aerated flow on a spillway of slope θ becomes fully developed, $\dot{V}=0$ and the mean air concentration attains its equilibrium value $\bar{C}_e$; the value of V_{en} can thus be evaluated as:

$$V_{en} = \bar{C}_e \, W \cos \theta \tag{3}$$

Assuming that V_{en} has approximately the same value for a partially-developed aerated flow allows Equation (2) to be expressed in the form:

$$\dot{V} = W \cos \theta \, (\bar{C}_e - \bar{C}) \tag{4}$$

The model developed by Wood used a different continuity relation

$$\frac{d}{dx} (q\bar{C}) = \dot{V} \tag{5}$$

with $\dot{V}$ as given by Equation (4). If the air concentration is defined in terms of the unit discharges of air and water (q_a and q) such that:

$$\bar{C} = \frac{q_a}{q_a + q} \tag{6}$$

then it can be shown that Equation (1) is the correct formulation of the continuity condition.

In both models the entrainment velocity V_{en} in Equation (2) was calibrated using Straub & Anderson's (1958) data and prototype measurements made by Cain & Wood (1981) on Aviemore Dam in New Zealand. The effective rise velocity of the bubbles was found to be about 0.4-0.5m/s. Overall, the models are fairly similar and capable of describing the development of self-aerated flows along spillways with varying vertical curvature but straight walls.

However, they do not give any direct information about the vertical distribution of air within the flow.

By re-analysing Straub & Anderson's data in detail, Wood (1984) found that the shape of the equilibrium concentration profile for a self-aerated flow depended only on the value of the mean concentration $\overline{C}_e$ (which in turn was determined by the channel slope). The profiles were described by the function:

$$C = \frac{9 \exp(- G \cos \theta)}{9 \exp(- G \cos \theta) + \exp(- G \cos \theta \, Y^2)} \tag{7}$$

where Y is the non-dimensional height above the bed

$$Y = y/y_{90} \tag{8}$$

and y_{90} is the level (measured normal to the channel) at which the air concentration is 90%. The following values of $\overline{C}_e$ and the non-dimensional parameter G cos θ were obtained by Wood from Straub & Anderson's measurements:

θ	$\overline{C}_e$	G cos θ
7.5°	0.137	9.05
15.0°	0.245	5.90
22.5°	0.302	4.92
30.0°	0.410	3.80
37.5°	0.560	2.65
45.0°	0.618	2.30
60.0°	0.675	1.90
75.0°	0.715	1.60

For a self-aerated flow, it may be reasonable to assume that, even if the flow has not reached the fully-developed equilibrium state, the vertical distribution of the air will still mainly be determined by the value of the local mean concentration $\overline{C}$. Thus, if one of the numerical models described above predicts a certain value of $\overline{C}$, the concentration profile can be estimated from Equation (7) using the value of G cos θ for which $\overline{C}_e$ is equal to $\overline{C}$.

2.3 Aerator spacing

Existing guidelines on aerator spacing are mostly based on model and prototype observations of the rate at which air concentration decreases with distance.

Results of model tests for San Roque Dam presented by Volkart & Chervet (1983) showed that downstream of an aerator the local air concentration near the bed decreased from about 50% to less than 10% in a distance of 15m, for flow velocities in the range 25-32m/s ; these were prototype values obtained by scaling the model measurements. It was found that the required spacing between aerators depended on the flow velocity in the spillway and not on the discharge intensity per unit width. It is possible that these results were subject to some scale effect because of the difficulty of producing the correct turbulence levels and bubble sizes in a model.

Semenkov & Lentjaev (1973) gave the following prototype loss rates for different types of channel:

Straight section	0.5-0.8% per metre
Concave section	1.2-1.5% per metre

Typical distances between aerators were suggested to be in the range 30-100m. The above loss rates can be compared with a summary of Russian data given by Prusza et al (1983):

Straight section	0.15-0.20% per metre
Concave section (bucket)	0.50-0.60% per metre
Convex section	0.15-0.20% per metre

A possible explanation of the differences is that while Semenkov & Lentjaev's values refer specifically to Bratsk Dam (with a slope of 51°), Prusza et al's data may apply to flatter slopes.

Hamilton (1984) suggested that the loss rate might be expected to be proportional to the local air concentration, ie

$$\frac{dC}{dx} = - \alpha C \tag{9}$$

Which leads to an exponential equation of the form:

$$C = C_o \exp[- \alpha (x - x_o)] \tag{10}$$

where C_o is the value of concentration at distance x_o along the channel. Data from Bratsk Dam on the decrease of air concentration along the invert of the spillway (C decreasing from 85% to 35% in 53m) gives, for example, a value of α = 1.7% per metre.

Falvey (1990) extended this concept by assuming that the loss rate would be proportional to the difference between the local mean air concentration $\bar{C}$ and the equilibrium value $\bar{C}_e$ for a similar fully-developed aerated flow. This resulted in the suggested formula:

$$\bar{C} = (\bar{C}_o - \bar{C}_e) \exp[-0.017 (x - x_o)] \tag{11}$$

Chanson (1989) developed the one-dimensional numerical model of Wood (1985), see Section 2.2, so as to be able to predict changes in air concentration downstream of spillway aerators. It was assumed that the air entrained by a floor aerator is dispersed upwards into the flow by the high pressures occurring in the re-attachment zone, and that the resulting vertical distribution of air is similar to that found with a fully-developed self-aerated flow (see Equation (7) and accompanying Table). Concentration profiles measured in a model of an aerator for Clyde Dam showed satisfactory agreement with equivalent self-aerated profiles in the upper spray region but more significant differences in the lower bubble region close to the floor. Chanson used the same continuity equation and entrainment function as Wood (Equations (5) and (4)) together with a suitable gradually-varied flow equation to compute changes in mean air concentration with distance. Comparison of the numerical model with laboratory measurements indicated that the effective rise velocity of the bubbles was between 0.01m/s and 0.16m/s.

A two-dimensional analytical solution of the diffusion/advection equation was developed by Cui (1985) and evaluated using air concentration profiles measured downstream of a model aerator. The partial differential equation was solved by splitting the solution into two parts : a General Function representing a steady-state profile to which the air concentration tends at an infinite distance downstream ; and a Particular Integral which describes the initial profile at the upstream end of the channel and which decays exponentially with distance along the channel. The Particular Integral consists of a rather complex infinite series with coefficients that are determined from a harmonic analysis of the initial concentration profile. The solution was assumed to apply only in the lower bubble region of the flow defined as $C \leq 60\%$ and not to the upper droplet region (see Section 2.2). The General Function was therefore chosen so as to give a constant value of $C = 60\%$ at the upper limit of the bubble region. Evaluating only the first two terms of the infinite series and choosing suitable values for the rise velocity of the air bubbles and the diffusion coefficient of the flow, Cui found quite reasonable agreement between the predicted and measured concentration profiles. However, the method is not very flexible because it cannot take account of self-aeration, bulking and spatial variations in flow velocity and diffusion coefficient. Cui's paper is in Chinese but a Portuguese translation by Campos (1986) is available.

3 Diffusion/advection equation

The diffusion/advection equation is found to govern a variety of problems that involve some physical quantity which is transported by a fluid flow whilst being subject to molecular or turbulent diffusion. Consider the fluxes of a quantity E into and out of the two-dimensional elemental volume IJKL shown in Figure 1. The fluid flow has velocity components u and v which produce fluxes $F_{x1} = (uE)\Delta y$ and $F_{y1} = (vE)\Delta x$ through sides IJ and IL respectively.

Random movements of the fluid particles (due to molecular vibrations or larger-scale turbulent eddies) cause a net flux of the quantity E from regions of high E to regions of low E. The resulting components of the flux are therefore $F_{x2} = -(D\partial E/\partial x)\,\Delta y$ and $F_{y2} = -(D\partial E/\partial y)\,\Delta x$ through sides IJ and IL respectively ; D is the diffusion coefficient of the fluid. The differences between the values of the fluxes entering the elemental volume (through IJ and IL) and leaving (through KL and JK) determine the rate at which E changes with time inside the volume, ie:

$$-\frac{\partial}{\partial x}\left(uE - D\frac{\partial E}{\partial x}\right)\Delta y\Delta x - \frac{\partial}{\partial y}\left(vE - D\frac{\partial E}{\partial y}\right)\Delta x\Delta y = \frac{\partial E}{\partial t}\Delta x\Delta y \qquad (12)$$

which (assuming that D is constant) leads to:

$$\frac{\partial E}{\partial t} + u\frac{\partial E}{\partial x} + v\frac{\partial E}{\partial y} + E\left(\frac{\partial u}{\partial x} + \frac{\partial v}{\partial y}\right) = D\left(\frac{\partial^2 E}{\partial x^2} + \frac{\partial^2 E}{\partial y^2}\right) \qquad (13)$$

If the fluid is effectively incompressible, the continuity equation gives:

$$\frac{\partial u}{\partial x} + \frac{\partial v}{\partial y} = 0 \qquad (14)$$

so that Equation (13) becomes:

$$\frac{\partial E}{\partial t} + u\frac{\partial E}{\partial x} + v\frac{\partial E}{\partial y} = D\left(\frac{\partial^2 E}{\partial x^2} + \frac{\partial^2 E}{\partial y^2}\right) \qquad (15)$$

This is the standard form of the diffusion/advection equation. If the conditions have reached a steady state, $\partial E/\partial t = 0$.

The parameter E can be a vector quantity such as, for example, the component of fluid momentum ρu in the x-direction, where ρ is the density of the fluid. In this case, Equation (15) becomes an equation describing forces produced by the fluxes of momentum. With the inclusion of additional pressure and body forces (P and Ω), Equation (15) is then equivalent to the x-component of the well known Navier-Stokes equation:

$$\frac{\partial u}{\partial t} + u\frac{\partial u}{\partial x} + v\frac{\partial u}{\partial y} = (\nu + \varepsilon)\left(\frac{\partial^2 u}{\partial x^2} + \frac{\partial^2 u}{\partial y^2}\right) - \frac{1}{\rho}\frac{\partial}{\partial x}(P + \Omega) \tag{16}$$

Corresponding results apply for the other components of momentum flux. The diffusion coefficient D can be separated into two parts : the kinematic viscosity ν due to molecular diffusion ; and the eddy viscosity ε due to turbulent diffusion.

The parameter E can alternatively be a scalar quantity, such as the concentration C of some chemical (eg salt) that is completely dissolved in the fluid. For such a steady-state problem, Equation (15) becomes:

$$u\frac{\partial C}{\partial x} + v\frac{\partial C}{\partial y} = D\left(\frac{\partial^2 C}{\partial x^2} + \frac{\partial^2 C}{\partial y^2}\right) \tag{17}$$

This same equation is often also applied to two-phase problems such as suspended sediment in water or air bubbles in water. In the case of suspended sediment, this is reasonable because values of C are usually small (of the order of 10^{-3} or less) so that the fluid can still be considered as being continuous. However, it is now necessary to take account of an additional flux of sediment concentration due to the fall velocity w of the particles. It is assumed that the particles move at the same velocity as the surrounding fluid except for an additional downward component due to their gravitational weight. This fall velocity is assumed to be constant implying that the drag and weight forces acting on the particles are at all points in equilibrium. Assuming the fall velocity to be at an angle of θ to the y-axis, Equation (17) becomes:

$$(u + w\sin\theta)\frac{\partial C}{\partial x} + (v - w\cos\theta)\frac{\partial C}{\partial y} = D\left(\frac{\partial^2 C}{\partial x^2} + \frac{\partial^2 C}{\partial y^2}\right) \tag{18}$$

Although this is not a dynamic equation, it does implicitly take account of the forces acting on the sediment particles. The appropriate value of the diffusion coefficient D may not be exactly equal to that used in the Navier-Stokes Equation (16) ($D = \nu + \varepsilon$) because the presence of the sediment particles may alter the turbulence characteristics of the fluid.

In the case of aerated flows, the bubbles have an upward velocity W determined by the balance between the buoyancy and drag forces. Therefore, most references on the subject start from a diffusion/advection equation equivalent to:

$$(u - W\sin\theta)\frac{\partial C}{\partial x} + (v + W\cos\theta)\frac{\partial C}{\partial y} = D\left(\frac{\partial^2 C}{\partial x^2} + \frac{\partial^2 C}{\partial y^2}\right) \tag{19}$$

For high-velocity flows, it is normally reasonable to assume that:

$$u >> W \tag{20.1}$$

$$v \approx 0 \tag{20.2}$$

$$\frac{\partial^2 C}{\partial y^2} >> \frac{\partial^2 C}{\partial x^2} \tag{20.3}$$

with the x-axis taken as being parallel to the slope of the channel. Equation (19) then becomes:

$$u\frac{\partial C}{\partial x} + W\cos\theta\frac{\partial C}{\partial y} = D\frac{\partial^2 C}{\partial y^2} \tag{21}$$

However, there are several problems with this formulation. Firstly, it treats the air-water mixture as though it were a continuous homogeneous fluid whereas the two phases are physically distinct and need to be considered separately. Secondly, expressing the equation in terms of the concentration C does not give the correct relationship between the flow rates of air and water. From Equation (6), it follows that the ratio of the two unit discharges:

$$\frac{q_a}{q} = \frac{C}{(1-C)} \tag{22}$$

The difference between C (as used in Equation (21)) and C/(1 - C) is negligible in the case of most suspended-sediment problems because C is usually small. However, in aerated flows, C can approach unity so large errors can occur. Thirdly, the presence of the air "dilates" the water and makes the meaning of the diffusion terms D and $\partial^2C/\partial y^2$ uncertain. Fourthly, a numerical solution of Equation (21) in finite-difference form is difficult because the number of steps in the y-direction needs to be varied according to the amount of bulking produced by the air.

An alternative description of the diffusion/advection process that avoids some of these problems is now considered. Figure 2a shows an aerated flow within an elemental volume IJKL measuring Δx by Δy. The x-axis is chosen to be parallel to the mean flow direction (so by definition v = 0). Now imagine the bubbles shrunk down to points and leaving only "solid" water within the "virtual" element IJ′K′L measuring Δx by Δz. Let there be N bubbles per unit volume of solid water, and let each bubble have an associated volume V. The ratio β between the volumes of air and water within the real element IJKL is therefore given by:

$$\beta = \frac{vol\ of\ air}{vol\ of\ water} = NV \tag{23}$$

The bubbles are assumed to move at the same speed as the water in the x-direction, but to have a rise velocity of W cos θ in the real element IJKL. Since the dimension Δy of the aerated flow and the corresponding dimension Δz of the non-aerated flow are related by:

$$\Delta y = (1 + \beta)\ \Delta z \tag{24}$$

the equivalent rise velocity W_e in the virtual element IJ′K′L is given by:

$$W_e = \frac{W}{(1 + \beta)} \cos\theta \tag{25}$$

The flux of air in the x-direction due to advection by the water is:

$$F_x = (u\beta)\Delta z \tag{26}$$

This shows that the diffusion/advection equation should be expressed in terms of β and not the concentration C. Since the air and water phases have the same velocity in the x-direction, it follows from Equations (22) and (23) that:

$$\beta = \frac{C}{1 - C} \tag{27}$$

The flux of air in the z-direction due to advection, diffusion and the rise velocity of the bubbles is given by:

$$F_z = (v\beta - D\frac{\partial \beta}{\partial z} + \frac{\beta}{(1 + \beta)} W\cos\theta)\ \Delta x \tag{28}$$

For steady-state conditions, the balance of air fluxes entering and leaving the virtual element IJ´K´L leads to the equation:

$$\frac{\partial}{\partial x}(u\beta)\ \Delta z\Delta x + \frac{\partial}{\partial z}(v\beta - D\frac{\partial \beta}{\partial z} + \frac{\beta}{(1 + \beta)} W\cos\theta)\ \Delta x\Delta z = 0 \tag{29}$$

Use of the continuity Equation (14) finally gives:

$$u\frac{\partial \beta}{\partial x} + \frac{W\cos\theta}{(1 + \beta)^2}\frac{\partial \beta}{\partial z} = D\frac{\partial^2 \beta}{\partial z^2} \tag{30}$$

This is the governing diffusion/advection equation that forms the basis of the numerical model described in Chapters 4 and 5.

Instead of solving Equation (30) directly, the model works by calculating the fluxes F_x and F_z entering and leaving each elemental volume. An explicit finite-difference scheme is used based on previous HR work on diffusion/advection problems. Referring to Figure 2b, the fluxes entering and leaving the box IJ´K´L are estimated from Equations (26) and (28) as follows:

$$F_x(i) = u(i, j).\ \beta(i, j).\ \Delta z \tag{31.1}$$

$$F_x(i + 1) = u(i + 1, j).\ \beta(i + 1, j).\ \Delta z \tag{31.2}$$

$$F_z(j - 1) = \frac{\beta(i, j - 1)}{[1 + \beta(i, j - 1)]}.W(i).\cos\theta.\Delta x - D(i, j - 1).[\beta(i, j) - \beta(i, j - 1)].\frac{\Delta x}{\Delta z} \tag{31.3}$$

$$F_z(j) = \frac{\beta(i,j)}{[1+\beta(i,j)]} \cdot W(i) \cdot \cos\theta \cdot \Delta x - D(i,j) \cdot [\beta(i,j+1) - \beta(i,j)] \cdot \frac{\Delta x}{\Delta z} \qquad (31.4)$$

Values of the flow velocity u and the diffusion coefficient D can therefore be varied both longitudinally and normal to the flow, but the values need to be determined independently and introduced in the finite-difference scheme.

Two boundary conditions are applied. At the invert of the channel (z=o), the normal component of the flux is zero so:

$$F_z(0) = 0 \qquad (32)$$

At the free surface ($z = J \Delta z$), the normal component of the flux is specified to be:

$$F_z(J) = \frac{\beta(i,J)}{[1+\beta(i,J)]} \cdot W(i) \cdot \cos\theta' \cdot \Delta x - V_{en}(i) \cdot \Delta x \qquad (33)$$

where V_{en} is the effective velocity at which air is entrained downwards through the free surface by turbulence (see Section 2.2).

Applying the continuity principle to the air fluxes entering and leaving the box IJ'K'L in Figure 2b, and assuming steady-state conditions, gives:

$$F_x(i) + F_z(j-1) = F_x(i+1) + F_z(j) \qquad (34)$$

If the air concentration profile is specified in terms of values of β at the upstream end of the channel (x=0), the finite-difference scheme defined by Equations (31) to (34) can be used to advance the solution down the channel. Thus, the new value of β at position (i+1, j) is found using known values of the various parameters at positions (i, j-1), (i, j) and (i, j+1).

The profiles of β determined by the program refer to the "virtual" non-aerated model (see Fig 2a). These can be expressed as profiles in the "real" aerated model by using Equation (24) to convert between Δz and Δy. Thus a value of β (i, j) which is at a level of z = (j-½) Δz above the invert in the "virtual" model occurs at a level of:

$$y = [(j - ½) - ½\,\beta(i,j) + \sum_{m=1}^{m=j} \beta(i,m)]\Delta z \qquad (35)$$

above the invert in the "real" model. If required the values of β can be converted into equivalent values of air concentration using the relation:

$$C = \frac{\beta}{(1+\beta)} \qquad (36)$$

Thus, although the diffusion/advection process is described by means of a "virtual" non-aerated model, the results relate to a "real" aerated flow and can therefore be calibrated against experimental measurements obtained from laboratory or field tests.

4 Program description

4.1 General

ADAM, which stands for Air Diffusion-Advection Model, is a program designed to model the transport and diffusion of air bubbles in turbulent open channel flows. It is a 2-D model which uses an explicit finite difference scheme to calculate air concentration profiles. The program is written in FORTRAN 77 and does not require any special external functions. It was developed using a personal computer (Compaq Deskpro 286) and in compiled form occupies approximately 70 kBytes of memory.

4.2 Stability of the numerical scheme

The simple explicit finite-difference scheme described by Equations (31) to (34) in Chapter 3 was used to solve Equation (30) and proved to be satisfactory. Explicit finite-difference schemes have the advantage of simplicity but normally require rather small computational steps in order to be stable. Therefore the number of steps needed by the scheme may prove too demanding in terms of computational requirements. Unstable solutions can occur if the step length normal to the flow is too large relative to the longitudinal step length. The two stability criteria adopted in the program to minimise the amount of numerical dispersion and define the longitudinal step length were:

$$\Delta x \leq c \, \frac{U(\Delta z)^2}{2 D_{max}} \quad and \quad \Delta x \leq c \, \frac{U(\Delta z)}{W_N} \tag{37}$$

where

Δx	step length in longitudinal direction
Δz	step length normal to flow direction
U	mean flow velocity
D_{max}	maximum value of the diffusion coefficient
W_N	component of the rise velocity of air bubbles normal to the spillway surface
c	coefficient (in the program c = 0.25)

The value of coefficient c was chosen after a number of test runs showed that the computed values of air concentration did not alter with a decrease in c. The scheme was found to be stable for c = 0.25.

4.3 Diffusion coefficient

As mentioned in Chapter 3, only the component of the turbulent diffusion flux ($D\partial^2\beta/\partial^2 z$) was considered in the model since the longitudinal component will normally be very much smaller. A quantitative expression of the vertical diffusion coefficient D based on the classical turbulence theory by Prandtl is given in French (1986):

$$D = k\, u_* \, z \, (1 - z/h) \tag{38}$$

where

k	von Karman coefficient ($k \approx 0.40$)
u_*	shear velocity
z	height above bed
h	total flow depth

It can be seen that D increases from zero at the bottom, reaches a maximum at half flow depth and decreases back to zero at the surface. This expression was obtained from studies involving diffusion of fluid momentum ; in the absence of suitable data it was initially assumed that the same result would also apply to the diffusion of air by water. Later a constant depth-integrated value of D was also introduced in the program as an alternative to a diffusion coefficient variable with depth. The appropriate constant value is found from Equation (38) to be:

$$D = 0.067\ h\ u_* \tag{39}$$

As described in Section 2.2, studies of fully developed aerated flows by Gangadharaiah et al (1970) suggested that a line of demarcation can be defined by the points of maximum velocity along the channel. Below this line lies the wall turbulent zone which can be subdivided into an inner and an outer layer. In the inner layer the eddy viscosity (or diffusion coefficient) varies approximately linearly whereas it remains fairly constant (at about $0.07\ h\ u_*$) in the outer layer, according to experimental results by Laufer (1954). Although some controversy exists on this matter, there is experimental evidence (Straub & Anderson, 1958) that the inner layer ceases to exist in many cases. This finding supports the use of Equation (39) which gives a constant value of the diffusion coefficient very similar to the one applying in the outer layer. It was found that, for most of the experimental data tested with the program, use of a constant value of D gave more satisfactory results than a variable one; Equation (39) was therefore adopted (see Chapter 5).

4.4 Rise velocity of air bubbles

The rise velocity of air bubbles is, with the diffusion coefficient and the air entrainment through the surface, an important parameter in the modelling of air concentration profiles. This was apparent from the sensitivity tests carried out for this study and mentioned later in Section 5.1.

In a liquid at rest the rise velocity of air bubbles depends on: the physical properties of the liquid, such as its density, viscosity and surface tension ; the acceleration due to gravity ; and the diameter of the air bubbles. The latter parameter is the most relevant one when considering diffusion of air in spillways.

In the program it was decided to take into account the effect of vertical curvature of the spillway on the rise velocity of air bubbles. This made it necessary to determine the rise velocity from first principles, as a balance of buoyancy and drag forces:

$$B = V\,(\,\rho - \rho_a\,)\,a \tag{40}$$

$$F = \tfrac{1}{2}\,\rho\,C_d\,AW^2 \tag{41}$$

where

B	net buoyancy force resulting from the external pressure gradient
V	volume of air bubble (assumed equal to the volume of the equivalent sphere)
ρ	density of water
ρ_a	density of air
a	resultant of the acceleration g due to gravity and the centripetal acceleration U^2/R due to spillway curvature (R is the vertical radius of curvature); for a constant channel slope, a = g
F	drag force
C_d	drag coefficient
A	cross-sectional area of bubble (assumed equal to the area of the equivalent sphere)
W	rise velocity of air bubble

The balance of the two forces gives:

$$W = \left(\frac{4da(\rho - \rho_a)}{3C_d\rho}\right)^{0.5} \tag{42}$$

where d is the equivalent bubble diameter.

Rao & Kobus (undated) presented a graph giving the relationship between bubble diameter and the rise velocity of single bubbles in still water. The data had been collected by Haberman & Morton (1954) using the results of various authors. The rise velocity of very small air bubbles increases rapidly with size but the increase is much slower for bubbles with diameters greater than approximately 0.3mm.

The graph due to Haberman & Morton for tap water was analysed in order to obtain a general method for estimating rise velocity from Equation (42). Haberman & Morton's curve for hydrostatic conditions (Figure 3) was subdivided into three distinct regions: region I, where the rise velocity increases rapidly with the bubble size; region II, where the variation of the rise velocity is so small that it can be fitted by a horizontal line; and region III, where the increase is again significant but slower than in region I. Each region of the curve was approximated by a straight line on the log-log plot. Region I corresponds to bubble sizes smaller than 0.4mm, region II to bubble sizes between 0.4 and 2.2mm, and region III to bubbles bigger than 2.2mm (see Figure 3).

It was then possible to find relationships for each region between the drag coefficient C_d and the Reynolds number of the air bubbles, defined as $R_e = Wd/v$. These relationships were introduced in Equation (42) to calculate W in the three different regions for given values of d and resultant acceleration a:

$$C_d = 0.62 \quad \text{for } R_e \geq 470 \tag{43}$$
$$C_d = 0.0011\, R_e^{1.03} \quad \text{for } 87.1 \leq R_e < 470 \tag{44}$$
$$C_d = 1.99\, R_e^{-0.65} \quad \text{for } R_e < 87.1 \tag{45}$$

The program also includes a subroutine which calculates R_e to check if the equation used is within the range of Reynolds number for which it is valid; if not, a new value of the rise velocity is calculated using the correct equation.

It might be expected that the bubble size would change with depth, as the bubble crosses regions of decreasing pressure on its rise to the surface. However, the bubble size has in fact been found to remain approximately constant (see Rao & Kobus).

For the computation of the effective rise velocity of air in chute spillways it is necessary to consider the component of the rise velocity normal to the spillway bed. This becomes increasingly important as the spillway becomes steeper. The program calculates the rise velocity allowing for changes in the geometry of the different reaches of the spillway.

It should be noted that air bubbles of different sizes are usually produced in natural air-water flows, and the rise velocity of an individual bubble is likely to be influenced by its neighbours. Difficulties in measuring bubble sizes have led to insufficient information on how to quantify that dependence. Rao & Kobus pointed out that diameters between 3 and 10mm have been observed in fully turbulent flows. Visual observation of aerated flows along model spillways has suggested sizes of 1 to 3mm according to Tan (in Low, 1986). Field measurements at Aviemore Dam spillway, New Zealand, taken by Cain and Wood (1981) revealed bubble sizes of about 0.5-3mm in the lower regions of the flow, for mean air concentrations below approximately 20%.

4.5 Air entrainment through the surface

In order to model changes in air concentration downstream of aerators it is necessary to take account of air entrainment at the surface, as discussed in Section 2.2. The process and amount of air entrainment is closely associated with the level of turbulence in the flow. Because turbulence has the effect of breaking up the water surface, it allows the engulfing of air into the flow (and also its release).

The concept of a velocity of entrainment V_{en} can be introduced to aid the modelling of this process. In the program, the flux of air at the surface was defined as the difference between the upward flux due to the rise velocity of the bubbles and the downward flux produced by the entrainment velocity (see Equation (33)). Ackers & Priestley (1985), using data obtained by Straub & Anderson for mean air concentrations in uniform flow, produced two graphs showing the dependence of the entrainment function ($\phi=V_{en}/W$) on the Froude number of the flow and on the channel slope. Ackers & Priestley assumed a constant value of W of 0.5m/s. The values of V_{en} suggested by these graphs were used in the development stages of the present program but unsatisfactory results were obtained.

It was therefore decided to calibrate V_{en} directly against the experimental results of Straub & Anderson (1958). This is described later in Chapter 5. It was found that V_{en} varies linearly with the mean velocity of the non-aerated flow. However, further study of the parameter's dependence on the flow conditions is required for a better description of the physical processes involved in air entrainment.

4.6 Structure of the program

The program ADAM is formed by a number of subroutines and is structured in order to allow interaction with the program CASCADE for designing aerators. Values of mean flow velocity, water depth, slope angle and radius of vertical curvature of the spillway are read in by subroutine INPUT for various positions along the spillway. These values can be supplied to ADAM by CASCADE. Knowing the mean flow velocities, the program calculates the velocity profiles using the following equation obtained by Cain & Wood (1981) from prototype measurements on Aviemore Dam:

$$u = U\,(z/h)^{1/6.3} \tag{46}$$

where

u local mean velocity at height z above the bed

U mean flow velocity

h total flow depth

As mentioned in Section 4.3, the program requires the value of the shear velocity for the calculation of the diffusion coefficient. The shear velocity is obtained by using the Karman-Prandtl equation for rough turbulent flow. Both the velocity profile and the diffusion coefficient are calculated in subroutine CALC.

The longitudinal step length along the spillway is also determined at this stage of the program by subroutine STEP. The smaller of the two values defined in Section 4.2 is adopted as the longitudinal step but the program imposes a maximum value of 1m that should not be exceeded. Unlike the normal step height which changes linearly with the water depth, the longitudinal step is kept constant during the computations. The normal step height is simply defined as the total flow depth divided by the number of steps chosen by the operator (a minimum of 10 steps is however recommended).

CASCADE provides values of mean velocity and water depth at intervals along the spillway, but ADAM generally uses much smaller longitudinal steps. Values at intermediate points are therefore calculated by subroutine INTERPOL using linear interpolation.

The rise velocity of air bubbles is estimated in subroutine RISE before the computation of fluxes takes place. Since it depends not only on the spillway geometry but also on the value of flow velocity, the rise velocity is calculated at each longitudinal step. As mentioned before (see Section 4.4), subroutine CHECK is called to calculate the Reynolds number of the air bubbles and, if necessary, compute a corrected value of the rise velocity.

The computation of fluxes and air concentrations is performed by subroutine COMP using the explicit finite-difference scheme described in Chapter 3. At the bed of the spillway the flux of air is taken as zero; as mentioned in the previous section, the flux at the surface is due to the difference between the rise velocity of the bubbles and the downward velocity of air entrainment.

The profiles of the air/water ratio β are first calculated for the "virtual" non-aerated flow and the levels z then converted into equivalent levels y in the "real" aerated flow.

The results of the program therefore consist of air concentration profiles and corresponding values of mean concentration at successive points along the spillway. These are output into a file called "SPAC.RES". When the air concentration at the bed of the spillway falls below 7%, the program gives a warning of likely cavitation damage to the spillway - at this location a new aerator needs to be introduced in the spillway.

4.7 Input requirements

The input to the program is from a data file called "SPAC.DAT" and all the values have a free format. A blank space or a comma should be introduced between values in the same line. "SPAC.DAT" consists of a minimum of seven lines containing information on: position along the spillway, initial value of non-aerated water depth, mean flow velocity of non-aerated flow, slope angles in degrees and values of vertical radius of curvature (R is negative for convex curves and positive for concave curves). The value of the roughness height of the spillway bed k_s, the estimated diameter of air bubbles (in mm) and the number of vertical steps are next introduced in the data file. ADAM also requires the value of the kinematic viscosity of water and the entrainment velocity at the free surface.

The initial concentration profile is also part of the input file ; values of the air concentration of the non-aerated flow are introduced for each step normal to the spillway. It should be noted that it will normally be necessary to obtain a "crushed" profile, ie non-aerated profile, when starting from a measured concentration profile. The procedure to obtain a "crushed" profile is described in Section 5.3.

5 Testing of the model

5.1 General considerations

Three types of test were performed to validate the numerical model: sensitivity tests to assess the stability of the numerical scheme; calibration tests to estimate values of rise velocity and entrainment velocity; and comparative tests of the program output with laboratory and prototype results. The first type of test was already mentioned in Section 4.2 and led to the criteria for the longitudinal step length adopted in the program. The experimental data due to Straub & Anderson (1958) were used for the calibration tests. Their measurements of self-aeration provided a good basis for estimating the entrainment velocity at the surface of the flow. Testing against other experimental and prototype data proved more difficult, since only a few suitable studies were identified.

Although some researchers have been able to measure air concentration profiles in model and prototype spillways, the information provided is normally limited, in particular regarding the air bubble size and the diffusion coefficient. Also only initial values of mean flow velocity and water depth are usually presented and therefore assumptions about the changes in these two quantities along the spillway have to be made.

The results of the program were compared with two laboratory studies of spillway aerators carried out by Cui (1985) and by Low (1986). Three tests by Cui and one test by Low were analysed and compared with the results from ADAM. Analysis of prototype data on self-aeration obtained by Cain &

Wood (1981) from Aviemore Dam, New Zealand, was also carried out and the measurements compared with the computed values. It should be noted that no aerator was installed in the spillway studied by Cain & Wood; to the knowledge of the authors, no prototype measurements of air concentration profiles downstream of aerators are yet available.

5.2 Calibration of the entrainment velocity - Straub & Anderson's data

The classical work by Straub & Anderson (1958) on self-aerated flows in open channels was used to calibrate the value of the entrainment velocity in the program. Their extensive tests were carried out in an artificially roughened channel for 8 different slopes, varying between 7.5° and 75°, and various discharges. Measurements of distribution of air concentrations were taken and plotted at a point 13.5m downstream of the inlet, where the flow was considered to have reached equilibrium. Straub & Anderson found two distinct regions in their profiles: an upper region formed mainly by water droplets that move independently of the underlying flow, and a lower region where discrete air bubbles are transported and diffused by the turbulent flow (see Section 2.2).

Program ADAM was run for some of Straub & Anderson's data corresponding to slopes of 7.5°, 15°, 30°, 45°, 60° and 75°, and velocities of the non-aerated flow between 5.3 and 14.2m/s. The initial air concentrations were set to zero, and both constant and variable diffusion coefficients were tested (Equations (38) and (39)). After a number of trials satisfactory agreement was obtained between computed and measured values, in particular with the constant diffusion coefficient. The results are presented in Figures 4 to 6 where the experimental data due to Straub & Anderson can be compared with the curves predicted by the numerical model.

The agreement is very good in terms of magnitude and shape within the lower bubble region where the diffusion/advection equation is valid. In each case the limiting point (level y_L and concentration C_L) at which the predicted profile deviated significantly from the measurements was found to be close to the position of the transition which Straub & Anderson identified between the bubble and droplet regions.

Above the transitional level (upper region) a diffusion/advection model can no longer estimate air concentration profiles correctly. This is due to the fact that the liquid phase is not continuous so that concepts like turbulent diffusion and the rise velocity of bubbles cannot be applied any more. The concentration C_L corresponding to each limiting point was obtained and plotted against the mean concentration of the predicted profile $\overline{C}$. It was found that C_L could be related to $\overline{C}$ by the following equation:

$$C_L = 1.08\ \overline{C} \tag{47}$$

This result enables the limit of validity of the computer predictions for the lower bubble region to be estimated. All the concentration profiles plotted in Figures 4 to 6 were obtained with the same value of rise velocity of 0.25m/s (equivalent to a bubble size of d = 3mm), but with the entrainment velocity V_{en} varied to give the best overall agreement for each test. Consideration of the entrainment mechanism suggests that V_{en} should depend primarily on the magnitude of the turbulent velocity fluctuations. For a given level of turbulence, V_{en} might therefore be expected to vary linearly with the mean flow velocity. Figure 7 shows a plot of the best-fit values of V_{en} versus the mean velocity U of the non-aerated flow (as used in the "virtual" computational model, see Chapter 3). The data are fitted satisfactorily by the equation:

$$V_{en} = 0.0164\ U - 0.0493 \tag{48}$$

It is apparent from Figure 7 that there is a limiting value of the mean flow velocity below which entrainment of air does not occur. For Straub & Anderson's data, this value is equal to approximately 3.0m/s. The existence of a minimum velocity for air entrainment has been identified by other researchers. Ervine et al (1980) carried out a study of the effect of turbulence on the rate of air entrainment in plunging jets, and found values of the minimum velocity varying between 0.8 and 2.5m/s for turbulence intensities between 8 and 1%. The previous HR experimental study on ramp aerators (May, Brown & Willoughby, 1991) also demonstrated linear relationships between the rate of entrainment and the mean flow velocity, with entrainment starting at velocities between 2m/s and 4m/s.

Figure 5 shows two curves calculated by the present program using a depth-varying diffusion coefficient given by Equation (38) and a constant depth-integrated value given by Equation (39). Both approaches are satisfactory but close to the channel bed the constant value of the diffusion coefficient allows a better prediction of the experimental results. This was generally observed for the other profiles tested and therefore it was decided to adopt a constant diffusion coefficient.

Findings from these calibration tests with Straub & Anderson's data were used in the simulations of other laboratory and prototype measurements described in the following Sections.

5.3 Cui's data

With the purpose of validating his analytical solution (see Section 2.3), Cui (1985) measured air concentrations in a laboratory flume downstream of a ramp aerator for three different slope angles of the flume. The flume was 15m long, 0.2m wide and 0.3m high, and the measurements were carried out with an electric resistivity probe and averaged over 3 seconds.

All the three tests performed by Cui for slopes of 0°, 30° and 49° were compared with the results given by the program. Since the program initially considers non-aerated depths of water (see Chapter 3), it was necessary to convert the initial concentration profiles given by Cui (which were given in terms of bulk water depth) into "crushed" concentration profiles. This was done by multiplying water depth intervals along the vertical by the corresponding mean water concentrations at those levels, ie by (1-C) where C is the air concentration. The new "crushed" profiles were then obtained and introduced in the input data file ; the values of water depth and mean flow velocity given by Cui were interpreted as corresponding to the non-aerated water values. Although the flow velocity was taken as constant, it is likely to have varied somewhat along the 4 to 6m of the flume where the concentrations were measured. This may partly account for the difficulties in matching Cui's experimental data.

Different values of the surface roughness of the flume were tried and a value of k_s = 0.5mm was finally adopted. As a first attempt to fit his data, values of the rise and entrainment velocities suggested by Straub & Anderson's data were used, ie W = 0.25m/s and V_{en} given by Equation (48). The results are plotted as dashed lines in Figures 8 to 10. As can be seen, the agreement between the suggested values and the experimental data is relatively good for slopes of 30° and 49° but it is not satisfactory for the slope of 0°. It can also be observed from the Figures that the calculated dashed curves show a worse agreement with the experimental values for sections close to the origin of the measurements. Cui's origin was taken at the point of reattachment of the jet from the ramp. The impact of the jet locally increases pressures along the floor of the channel and causes the vertical pressure gradient to be greater than hydrostatic; this in turn increases the buoyancy and rise velocity of the bubbles. This effect can be simulated in the model by specifying a local region of concave curvature around the impact point. This procedure was used with Cui's data in order to obtain satisfactory fit; the bubble size and entrainment velocity had also to be adjusted.

Concave flow curvature with a radius of 0.5m was specified to apply over the first 0.5m of the channel downstream of the re-attachment point. The results obtained are plotted as solid lines in Figures 8 to 10. The values of bubble size, rise velocity (hydrostatic conditions) and entrainment velocity that gave the best agreement were as follows:

Slope	Bubble size (mm)	Rise velocity (m/s)	Entrainment velocity (m/s)
0°	8	0.41	0.05
30°	3	0.25	0.08
49°	3	0.25	0.15

For comparison, the dashed lines in Figures 8 to 10, based on Straub & Anderson's data and no flow curvature, assumed a 3mm bubble size and entrainment velocities of 0.11m/s, 0.07m/s and 0.085m/s (for the slopes of 0°, 30° and 49° respectively).

It can also be seen from the figures that the relationship between C_L and $\overline{\tau}$ found for Straub & Anderson's data (Equation (47)) is approximately valid for Cui's data. For example, for the slope of 30° and a section 4.37m downstream of the origin, C_L given by equation (47) is around 10% ; from the graph it is about 7.5%.

5.4 Low's data

Low (1986) obtained a series of air concentration profiles from measurements downstream of an aerator (ramp and offset) in a 1:15 scale model of the Clyde Dam Spillway, New Zealand. The slope of the spillway was 51.34°. One of his tests (Run 31) was chosen for comparison with the numerical model. The procedure adopted for Cui's data, described in the previous section, was also used for Low's results in order to obtain the velocity and flow depth of the non-aerated profile. The initial air concentration profile was taken 0.309m downstream of the point of reattachment of the jet and the mean flow velocity used in the calculations was 8.72m/s at that section. An estimate of the velocity at the end of the flume was also made and a linear variation with distance assumed to apply.

A good fit was achieved for a roughness coefficient of 0.1mm, rise velocity of 0.36m/s and entrainment velocity of 0.096m/s. The results are presented in Figure 11.

As before, Figure 11 shows dashed lines which correspond to the values of $W = 0.25$m/s and $V_{en} = 0.094$m/s suggested by Straub & Anderson's data, and solid lines which correspond to the best fit curve. Because the origin of the profiles was taken some distance downstream of the impact point of the jet, it was not necessary to specify any flow curvature in the spillway. For the profile at 1.214m downstream from the origin, C_L given by Equation (47) would correspond to 18% ; in Figure 11 it can be seen to be approximately 22%.

5.5 Cain and Wood's data

Cain & Wood (1981) carried out a series of measurements of air concentrations on the spillway of Aviemore Dam, New Zealand. The measurements were taken at five stations along the spillway (slope 45°), downstream of the inception point, for two different gate openings : 300 and 400mm. It was decided to use for the present analysis the results obtained for a gate opening of 300mm, which corresponded to a specific discharge $q = 2.23\text{m}^2/\text{s}$.

For computation purposes, the air concentration at the inception point was taken as zero. As before, the non-aerated depths at the different stations had to be determined from the measured profiles in order to obtain mean flow velocities. These values of non-aerated flow velocities were then introduced in the program and predicted concentration profiles obtained for stations 503 (19.89m downstream of the inception point) and 505 (32.08m downstream of the inception point). They are plotted with a solid line in Figure 12 for comparison with the curves drawn through Cain & Wood's measurements. A reasonable fit was achieved with V_{en} = 0.20m/s and W = 0.23m/s whereas Straub & Anderson's results would suggest V_{en} = 0.19m/s and W = 0.25m/s. As can be seen, these two sets of values are very similar. The agreement is also satisfactory in terms of the limiting concentration C_L. In fact, in Figure 12 C_L is approximately equal to 50% and 58% for stations 503 and 505, respectively ; the predicted values using Equation (47) would give C_L equal to 40% and 49% for stations 503 and 505.

6 Conclusions and recommendations

(1) A two-dimensional numerical model (called ADAM) has been developed for predicting changes in air concentration downstream of aerators in chute spillways. The model also simulates the effect of self-aeration at the free surface. Existing one-dimensional models can only estimate how the depth-averaged air concentration varies with distance. ADAM is also able to predict the distribution with depth, and so gives values of air concentration along the invert of the channel. This information is needed when identifying where aerators should be located on spillways in order to prevent cavitation damage.

(2) ADAM describes the behaviour of aerated flows in terms of the diffusion/advection (DA) equation, which previous experimental studies have shown to be appropriate. However, theoretical and practical problems arise when applying the DA equation to two-phase flows where the proportions of the two phases are of similar magnitude. In ADAM, the equation is first solved in terms of a "virtual" non-aerated flow and the results then transformed into values for the equivalent aerated flow.

(3) The DA equation only applies in the lower region of an aerated flow where the mixture consists principally of air bubbles in water. Results from ADAM are therefore not valid in the upper region consisting mainly of water droplets in air. Although air concentration profiles in the upper region have been found to follow a Gaussian-type distribution, the fundamental governing equation has not yet been satisfactorily

established. Fortunately, the lower region in which ADAM applies is of main importance because it is the region in which cavitation damage can occur.

(4) The model takes account of bubble size, spillway slope, spillway curvature and spatial variations in flow velocity. Tests were made to investigate alternative assumptions about the coefficient of diffusion for aerated flows. Satisfactory results were obtained using a depth-averaged value equal to that for momentum diffusion in an equivalent non-aerated flow.

(5) Self-aeration at the free surface is described in ADAM in terms of an entrainment velocity which is equal to the downward flow rate of air per unit surface area. Calibration of the model against Straub & Anderson's (1958) laboratory data gave consistent results and indicated that the entrainment velocity increases linearly with the mean velocity of the water flow.

(6) ADAM was tested against data from two model studies of spillway aerators and one field study of self-aeration in a prototype spillway. Reasonable agreement was obtained but assumptions were necessary because the experimental data did not give sufficient information on factors such as bubble size, surface aeration, and vertical and longitudinal variations in velocity.

(7) Although the DA equation gives only a simplified description of the processes governing self-aerated flows, its application in ADAM has highlighted the current lack of information about the following factors:

- typical bubble sizes in high-velocity flows
- relationship between bubble size and effective rise velocity in turbulent flows with high air concentrations
- diffusion coefficients for aerated flows
- initial distribution of air within flow just downstream of aerators
- additional air entrainment at surface caused by presence of aerators
- effect of flow curvature in reattachment zones downstream of aerators

(8) The program in ADAM is written so as to make use of data generated by the CASCADE model for designing spillway aeration systems. Some

extra development work is necessary to integrate the two models and produce a single design package.

7 Acknowledgements

This study was carried out in the Research Department of HR Wallingford headed by Dr W R White. Assistance with the finite-difference scheme used in the numerical model was provided by Dr A J Cooper.

8 References

Ackers P and Priestley S J (1985). Self-aerated flow down a spillway. Proc of 2nd Int Conf on The Hydraulics of Floods & Flood Control, Cambridge, England.

Borden R C, Colgate D, Legas J and Selander C E (1971). Documentation of operation, damage, repair and testing of Yellowtail Dam spillway. Bureau of Reclamation Report No REC-ERC-71-23.

Cain P and Wood I R (1981). Measurements of self-aerated flow on a spillway. Journal of the Hydraulic Division, Proc ASCE, Vol 107, No 11, pp 1425-1444.

Campos J A P (1986). Distribuicao da concentracao de ar a jusante de uma rampa de arejamento. Translation from Cui (1985) paper. Traducao 825, LNEC, Lisbon, (in Portuguese).

Chanson H (1989). Flow downstream of an aerator - aerator spacing. Journal of Hydraulic Research, Vol 27, No 4, pp 519-537.

Colgate D and Elder R (1961). Design considerations regarding cavitation in hydraulic structures. Tenth Hydraulics Division Conference, ASCE, Urbana, IL.

Cui L T (1985). Air concentration distribution downstream of aeration ramp. Journal of Hydraulic Engineering, No 1, Beijing, (in Chinese).

Ervine D A, McKeogh E and Elsawy E M (1980). Effect of turbulence intensity on the rate of air entrainment by plunging water jets. Proc ICE, Part 2, Research and Theory, Vol 69, pp 425-445.

Falvey H T (1990). Cavitation in chutes and spillways. Engineering Monograph No 42, US Department of the Interior, Bureau of Reclamation.

French R H (1986). Open-channel hydraulics. McGraw-Hill Book Company, Singapore, ISBN 0-07-Y66342-4.

Gangadhariah T, Lakshmana Rao N S and Seetharamiah K (1970). Inception and entrainment in self-aerated flows. Journal of the Hydraulics Division, Proc ASCE, Vol 96, No 7, pp 1549-1565.

Haberman W L and Morton R K (1954). An experimental study of bubbles moving in liquids. Proc ASCE, Engineering Mechanics Division, Vol 80, Separate No 387, pp 387-1 to 387-24.

Hamilton W S (1984). Preventing cavitation damage to hydraulic structures. Water Power & Dam Construction, Vol 36, (Part 3) January, pp 42-45.

Henderson F M (1966). Open channel flow. Macmillan Publishing Co, Inc. New York.

Laufer J (1954). The structure of turbulence in fully developed pipe flow. National Advisory Committee for Aeronautics, Washington DC, NACA. Technical Report No 1174.

Low H S (1986). Model studies of Clyde Dam spillway aerators. Research Report 86-6, Department of Civil Engineering, University of Canterbury, Christchurch, New Zealand.

May R W P (1987). Cavitation in hydraulic structures: occurrence and prevention. HR Report SR 79.

May R W P and Deamer A P (1989). Performance of aerators for dam spillways. HR Report SR 198.

May R W P, Brown P M and Willoughby I R (1991). Physical and numerical modelling of aerators for dam spillways. HR Report SR 278.

Pinto N L de S, Neidert S H and Ota J J (1982). Aeration at high velocity flows. Water Power & Dam Construction, Vol 32, (Part 1), February, pp 34-38 ; (Part 2) March, pp 42-44.

Pinto N L de S (1991). Air entrainment in free-surface flows - Chapter 5. Edited by Wood I R. A A Balkema, Rotterdam/Brookfield.

Prusza Z V, Mantellini T P and Semenkov V (1983). Remedial measures against spillway cavitation. Proc XXth IAHR Congress, Moscow, Vol 3, pp 468-476.

Rao N S L and Kobus H E (undated). Characteristics of self-aerated free-surface flows. Water and Waste Water. Current Research and Practice. Erich Schmidt Verlag, Germany, ISBN 3 503 013172.

Semenkov V S and Lentjaev L D (1973). Spillway dams with aeration of flow over spillways. 9th ICOLD Congress, Madrid, Separate Paper.

Straub L G and Anderson A G (1958). Experiments on self-aerated flow in open channels. Journal of the Hydraulics Division, Proc ASCE, Vol 84, No 7, pp 1890-1 to 1890-35.

Volkart P and Chervet A (1983). Air slots for flow aeration: determination of shape, size and spacing of air slots for the San Roque Dam Spillway. Mitteilungen der Versuchsanstalt für Wasserbau, Hydrologie und Glaziologie, ETH, Zürich, Nr 66.

World Water (1979). Cavitation casts doubt on Karun spillway design. June 1979.

Wood I R (1984). Air entrainment in high speed flows. Symposium on Scale Effects in Modelling Hydraulic Structures, Esslingen am Neckar, Germany, pp 4.1-1 to 4.1-7.

Wood I R (1985). Air water flows. Proc XXI st IAHR Congress, Melbourne, Vol 6, pp 18-29.

Figures

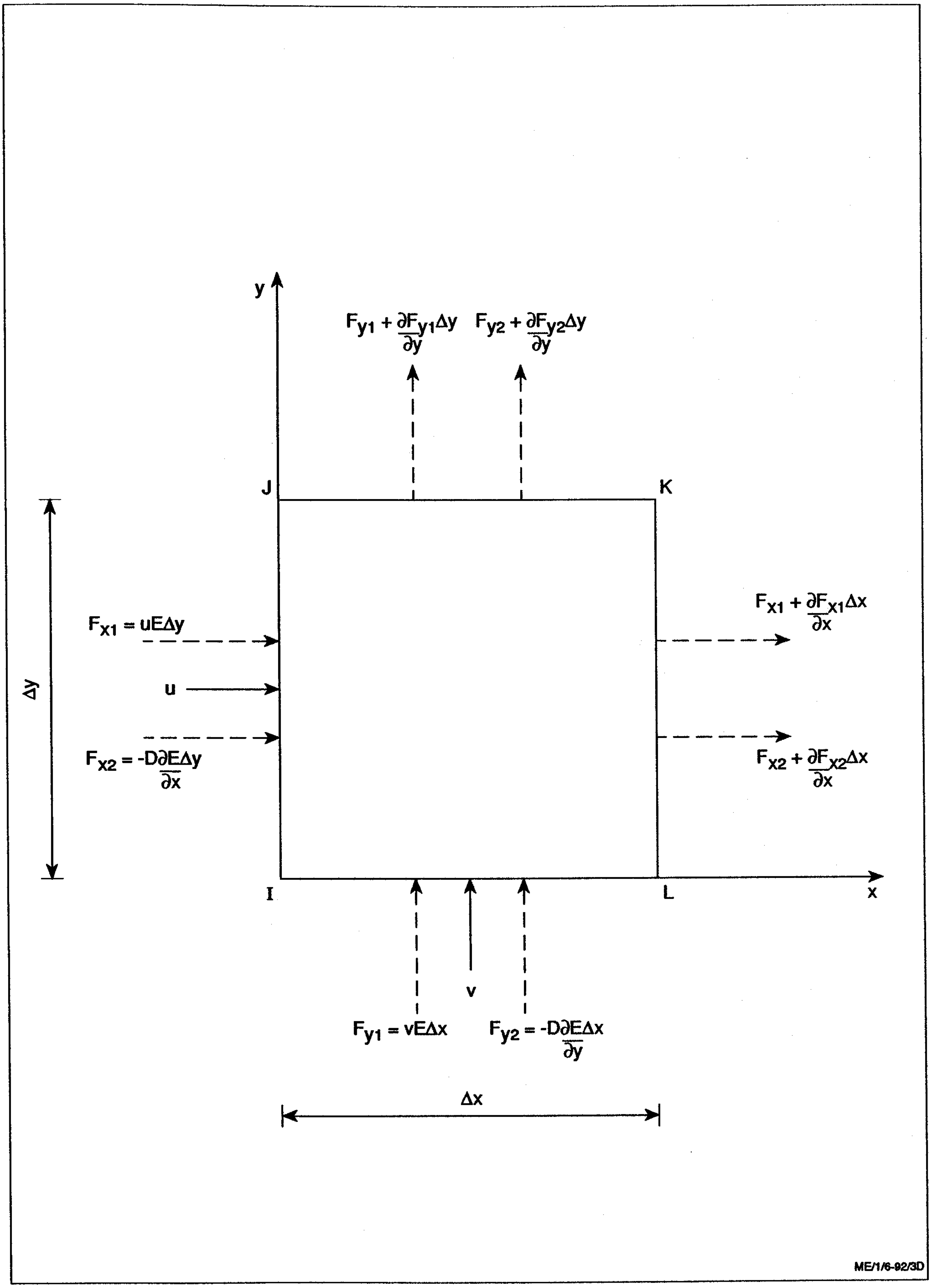

Figure 1 Fluxes of quantity E due to advection and diffusion

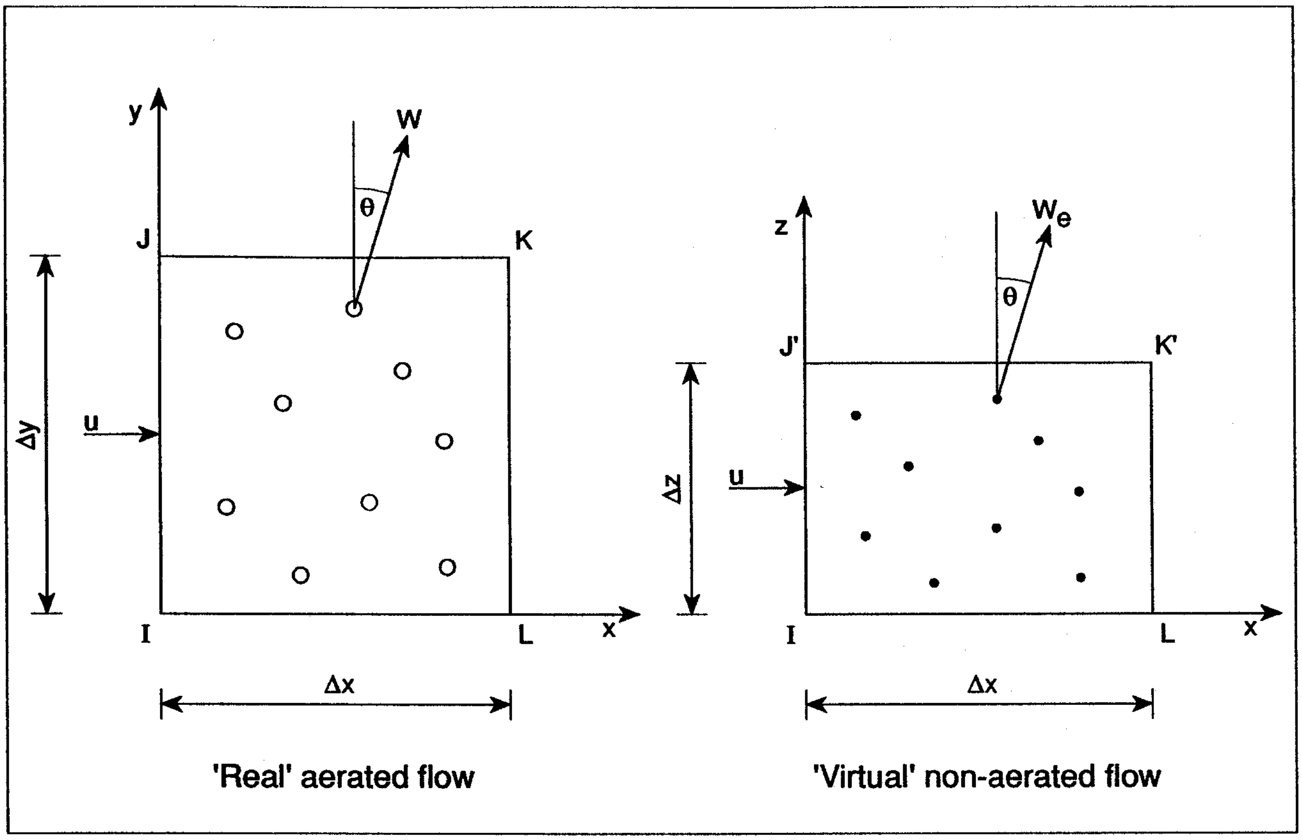

Figure 2a Definition of virtual model

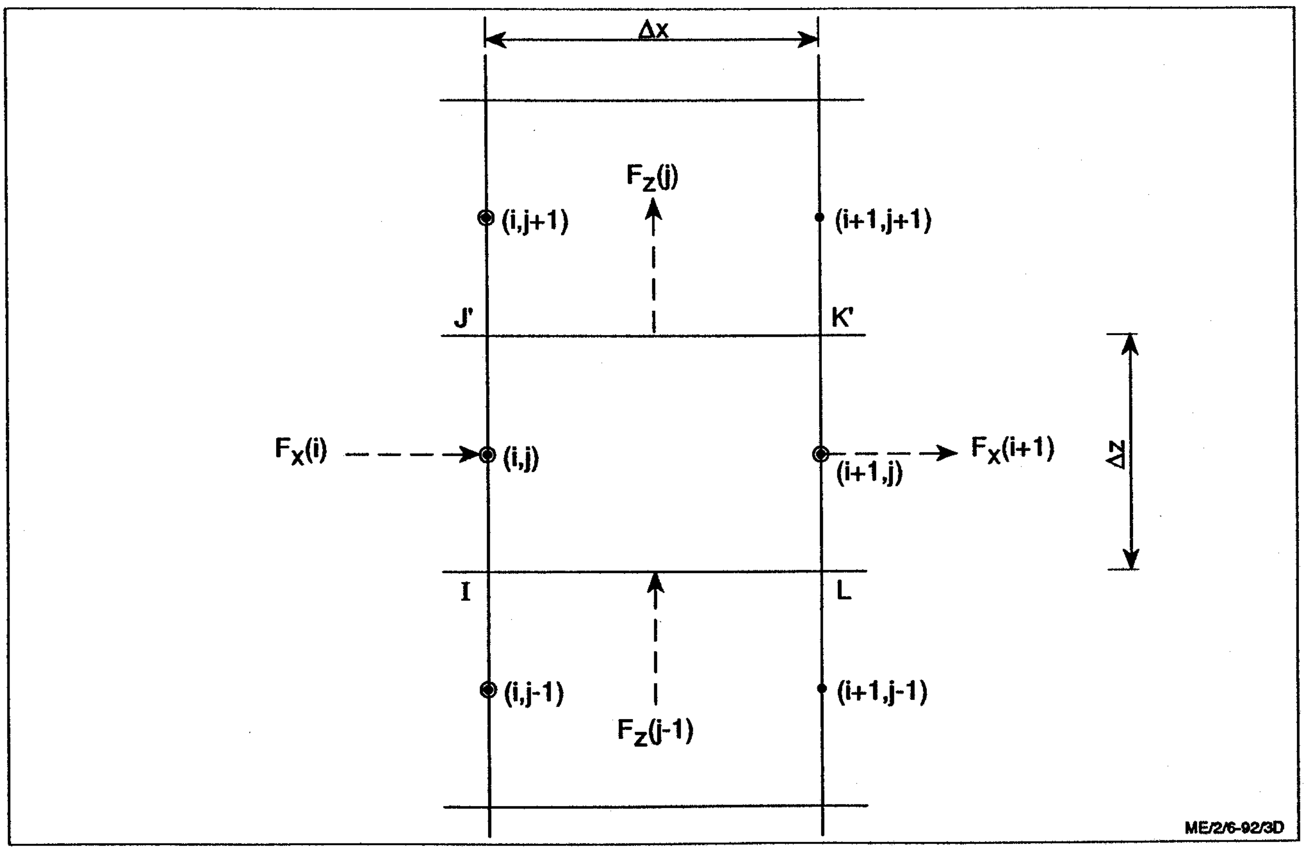

Figure 2b Finite difference scheme for model

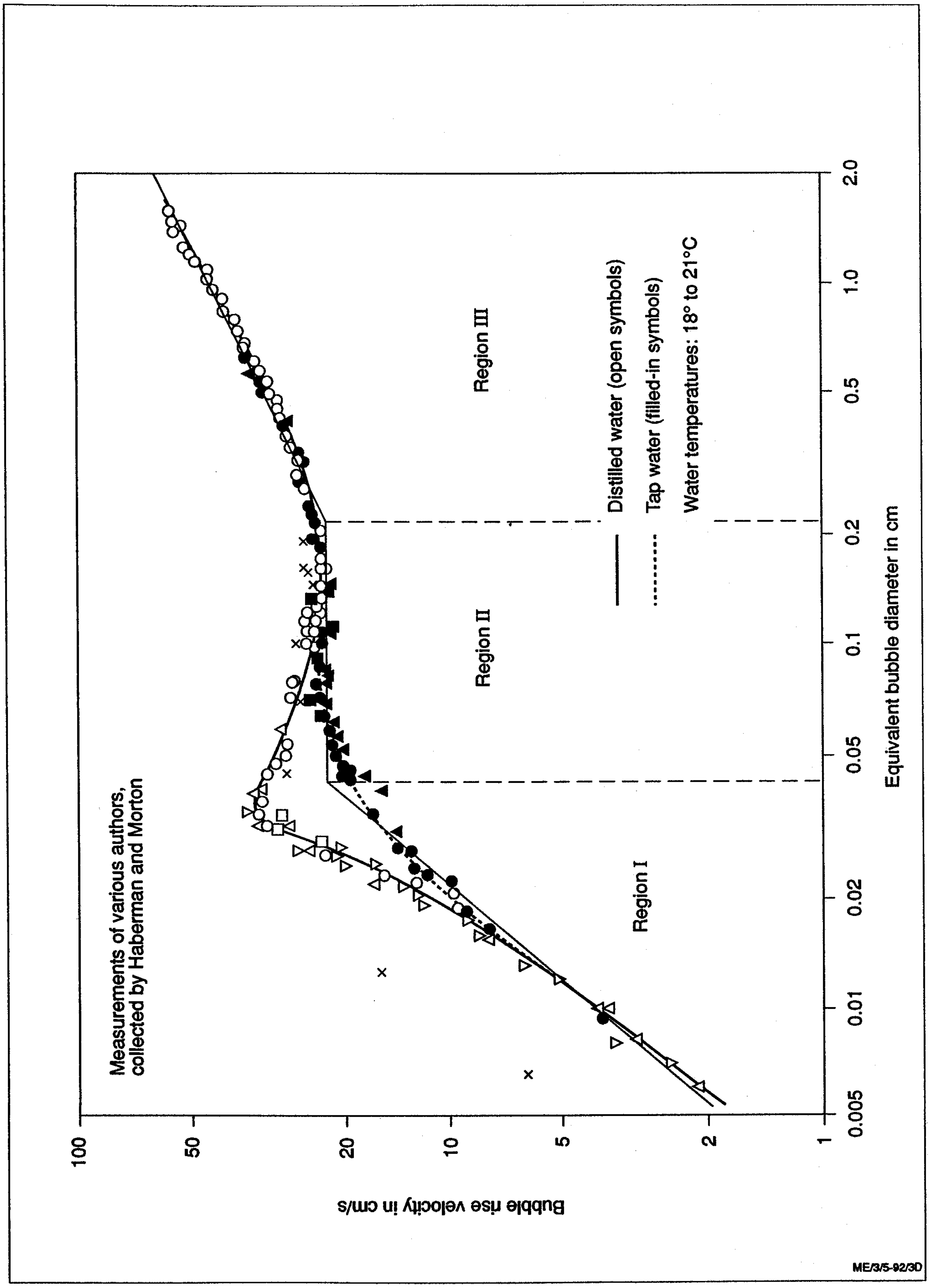

Figure 3 Relationship between air bubble diameter and rise velocity (from Rao and Kobus)

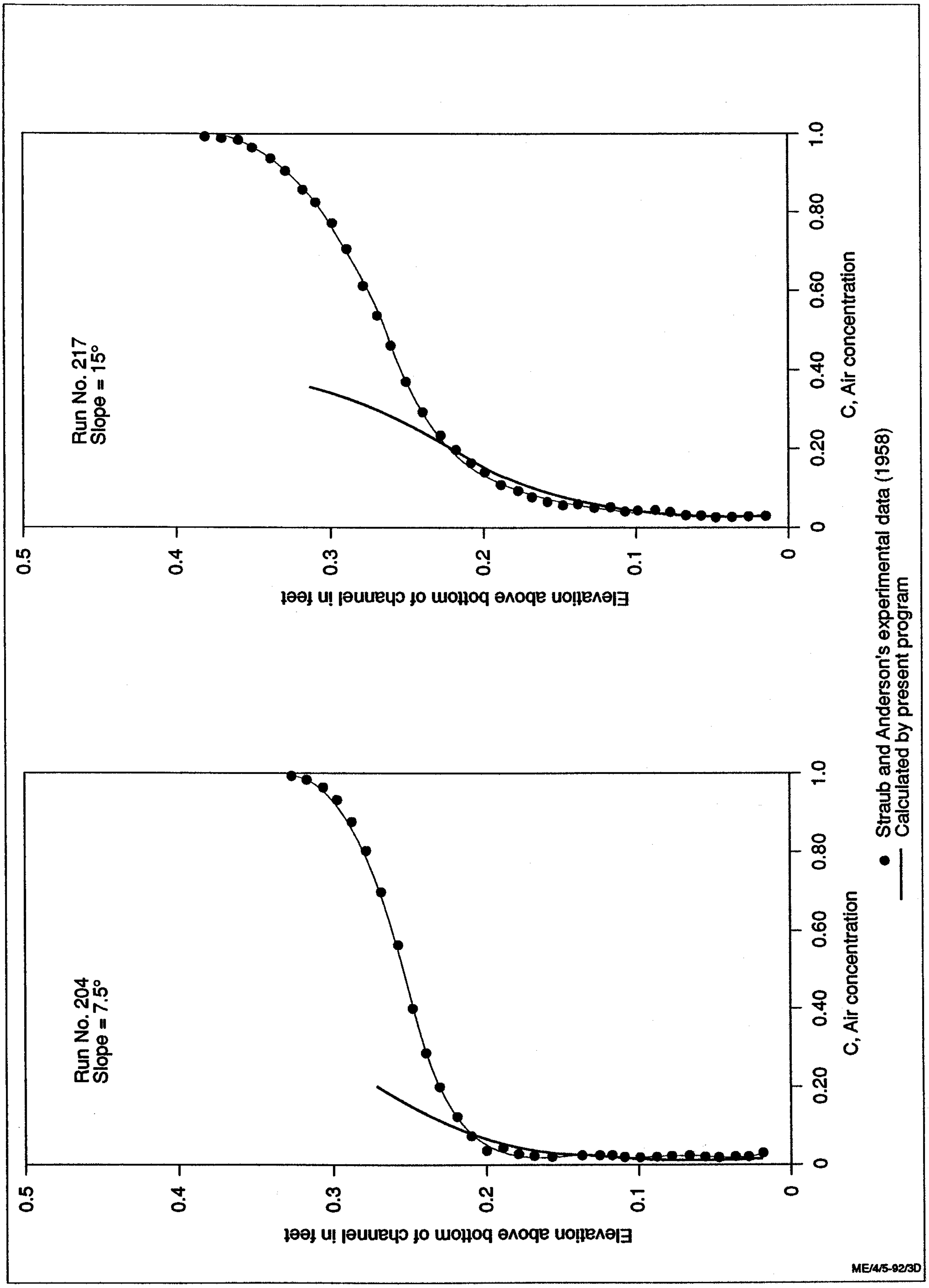

Figure 4 Comparison of calculated air concentration profiles with experimental results by Straub and Anderson for slopes 7.5° and 15°

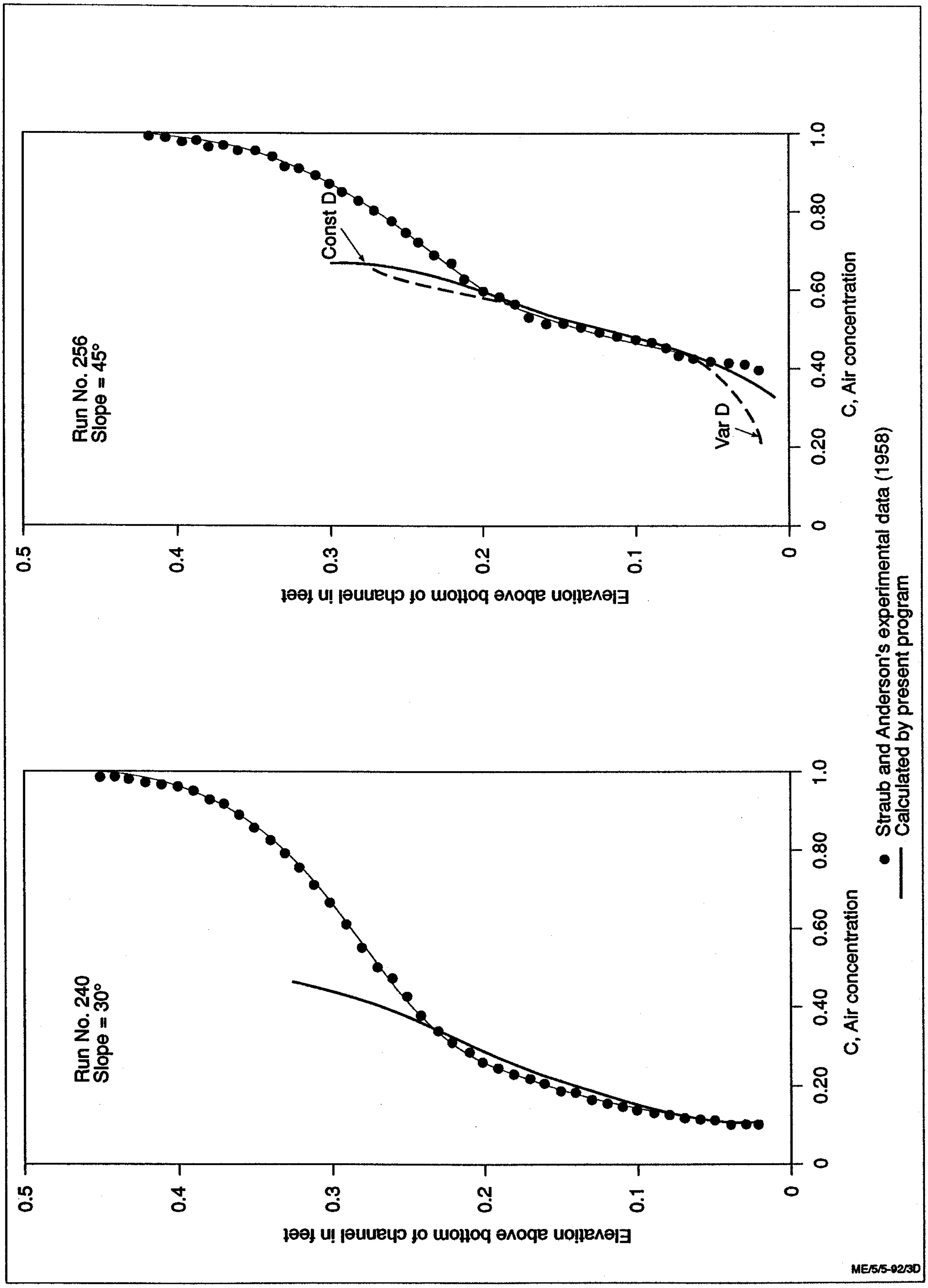

Figure 5   Comparison of calculated air concentration profiles with experimental results by Straub and Anderson for slopes 30° and 45°

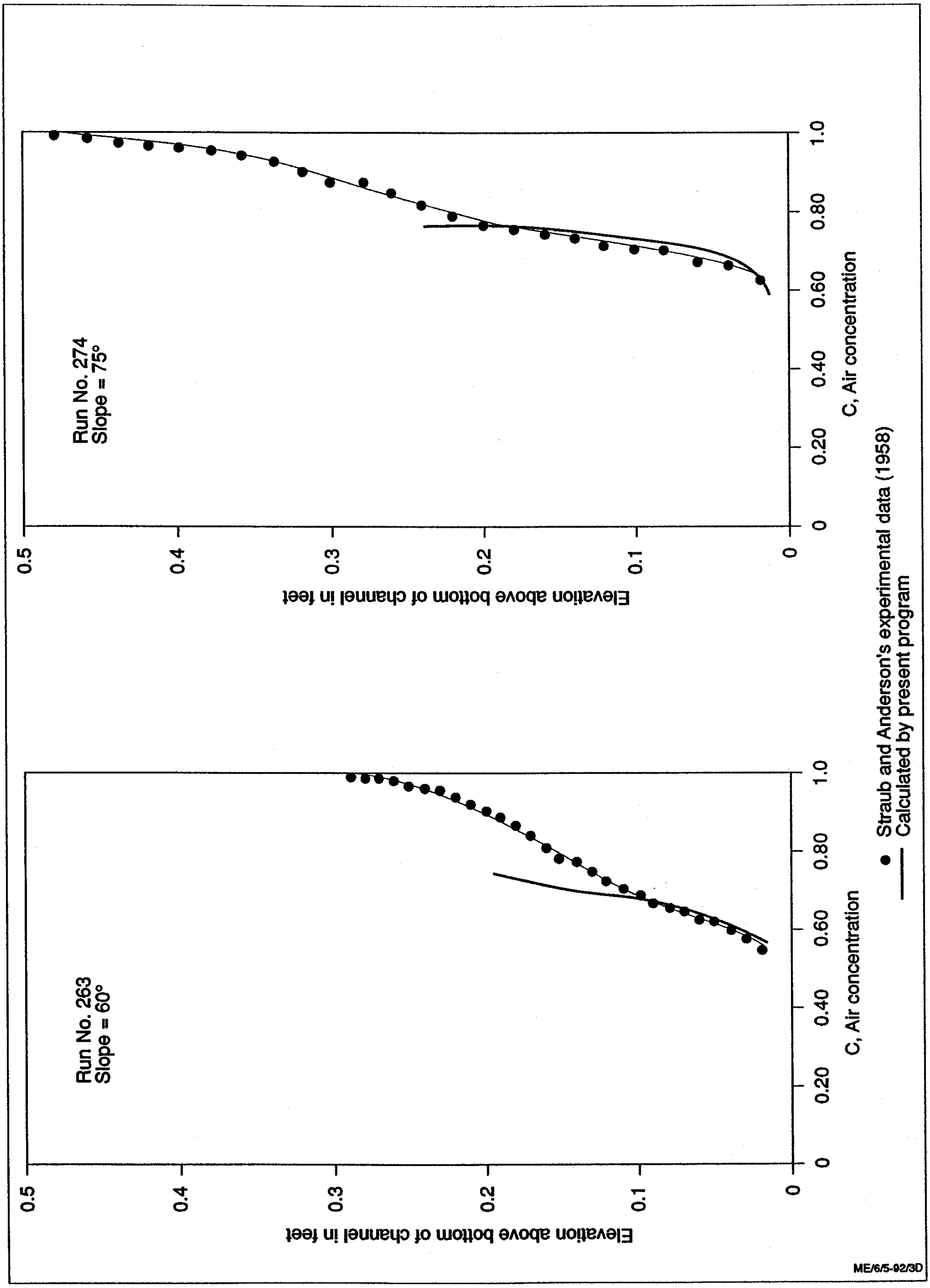

Figure 6 Comparison of calculated air concentration profiles with experimental results by Straub and Anderson for slopes 60° and 75°

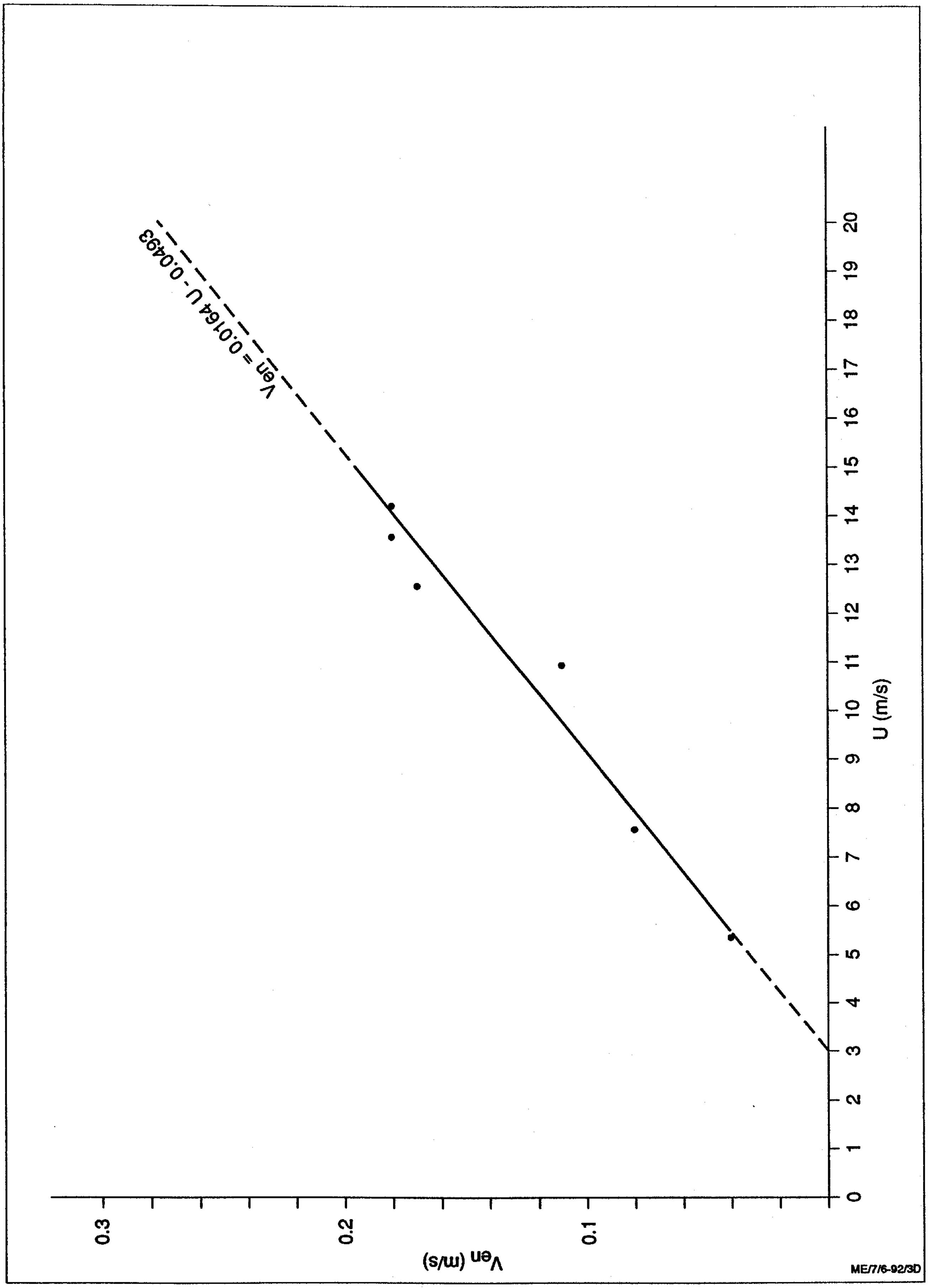

Figure 7   Relationship between mean flow velocity and entrainment velocity

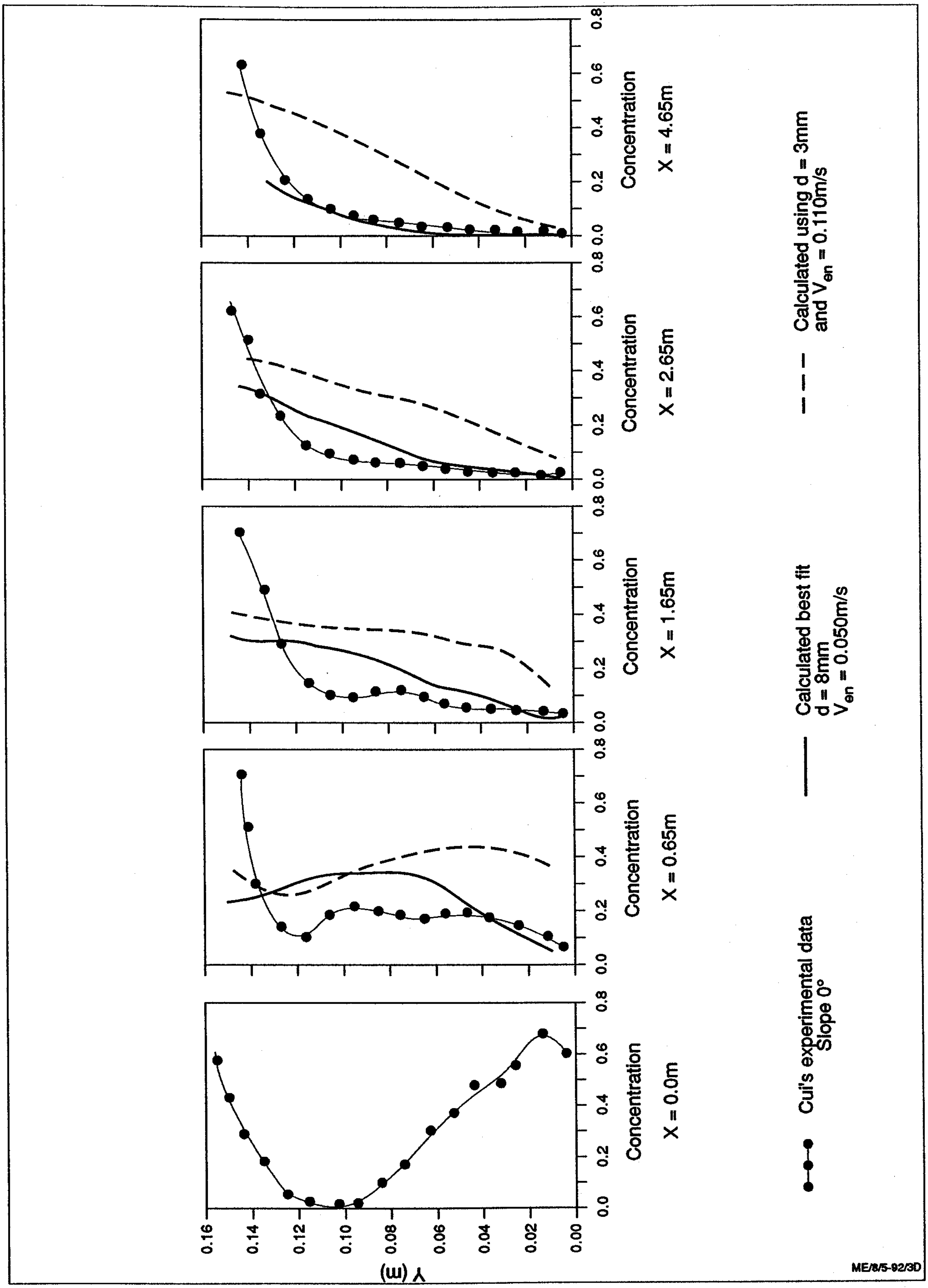

Figure 8 Comparison of calculated air concentration profiles with Cui's experimental results for slope 0°

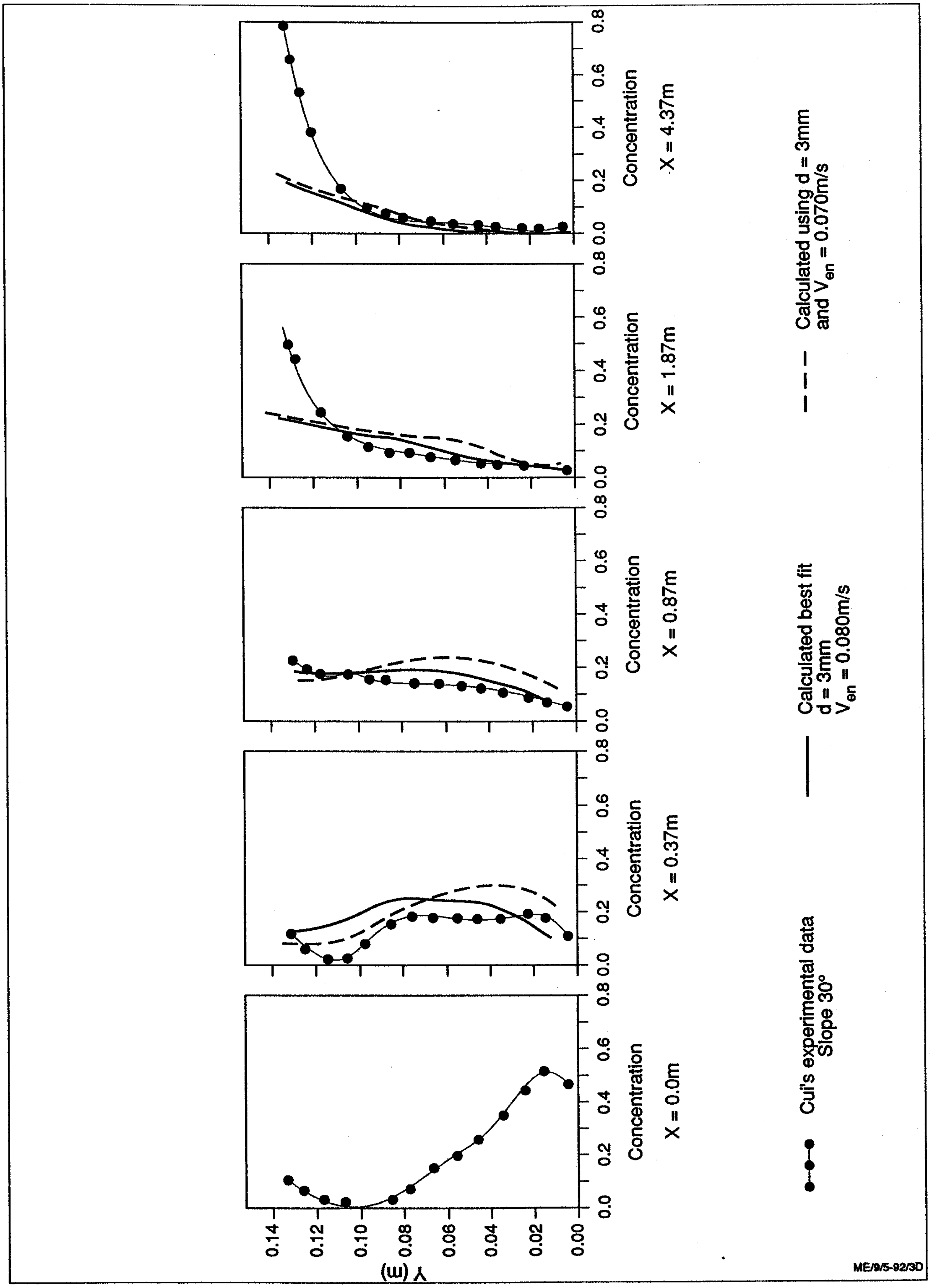

Figure 9 Comparison of calculated air concentration profiles with Cui's experimental results for slope 30°

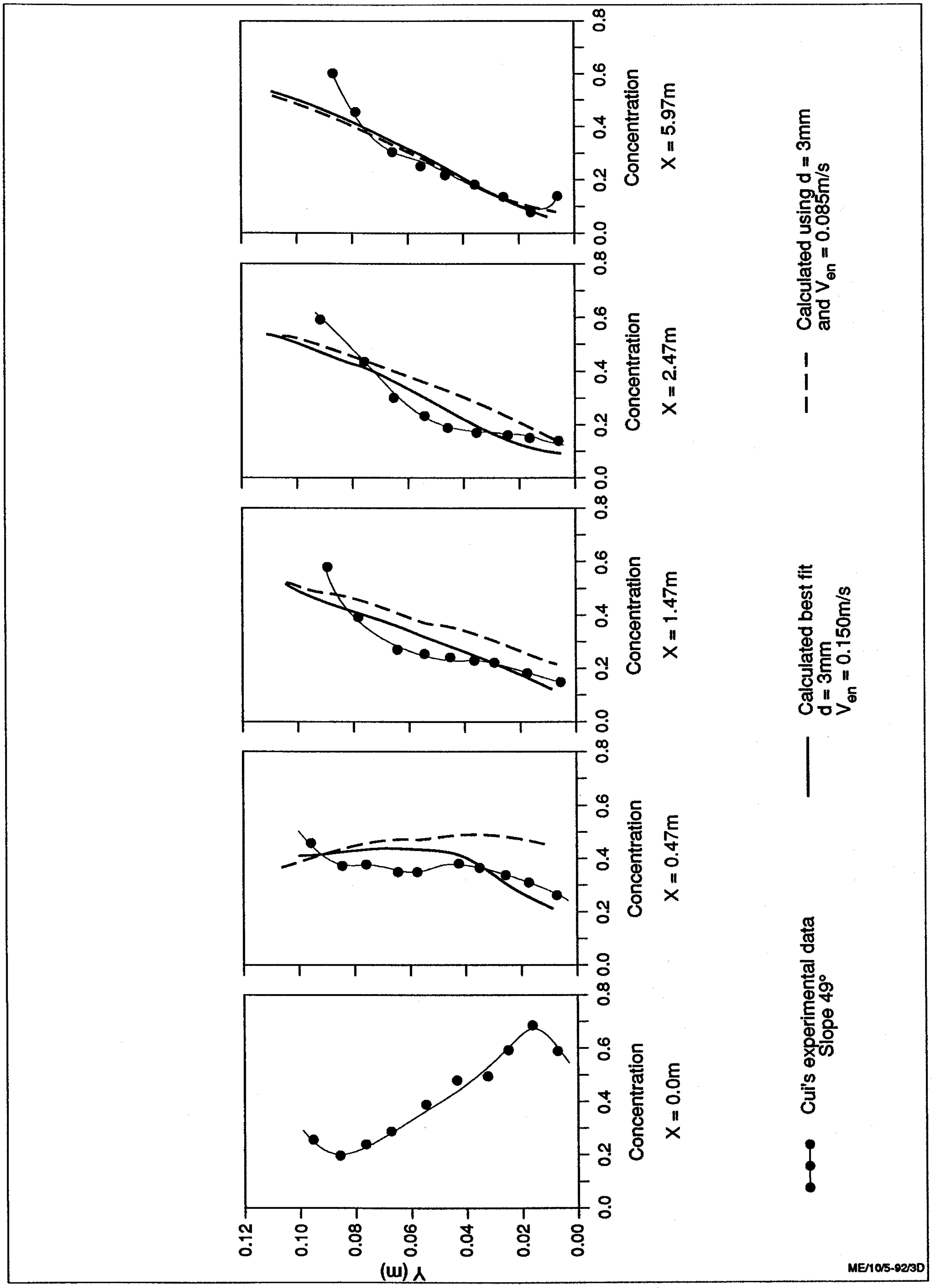

Figure 10 Comparison of calculated air concentration profiles with Cui's experimental results for slope 49°

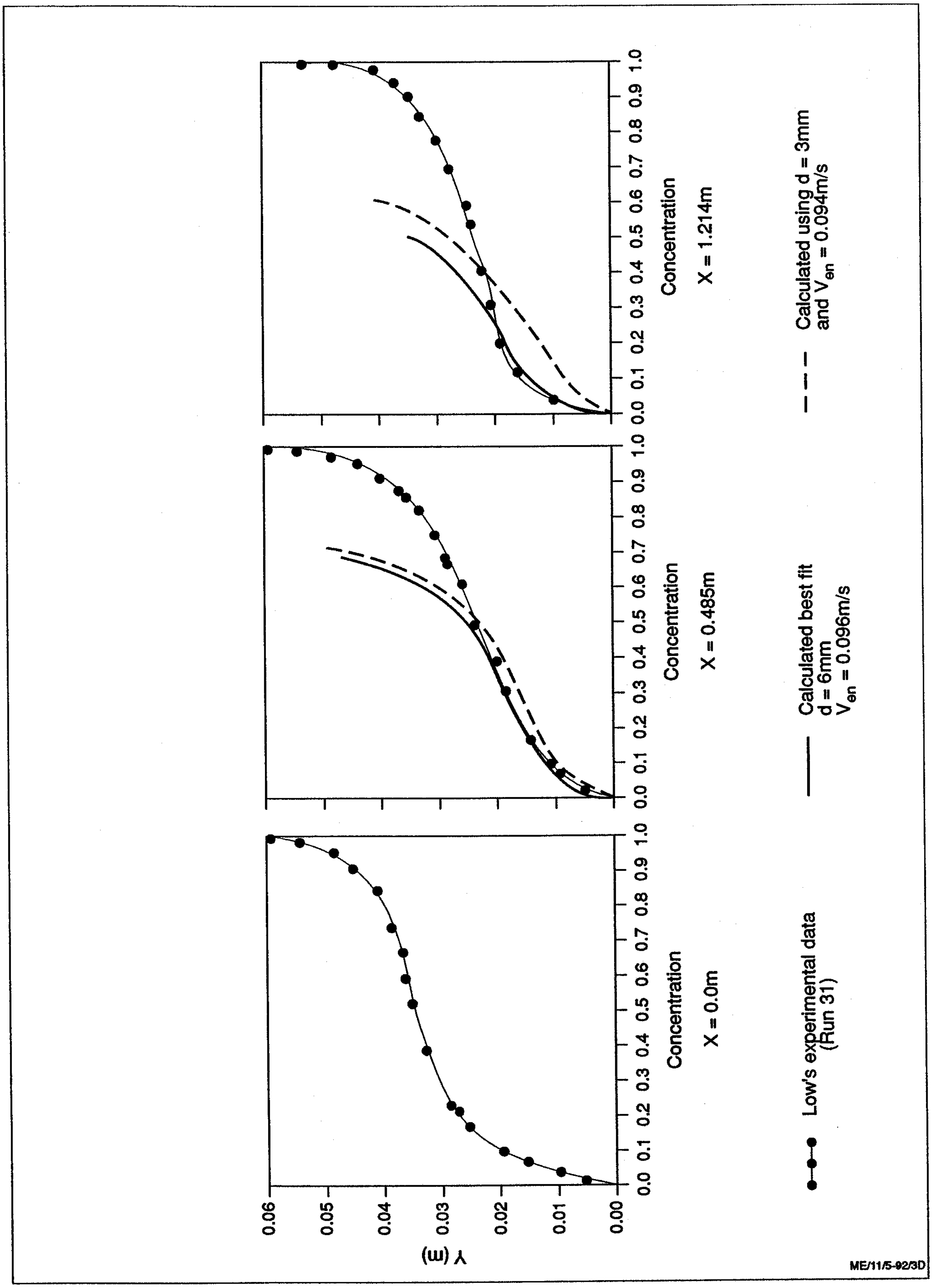

Figure 11 Comparison of calculated air concentration profiles with Low's experimental results (Run 31)

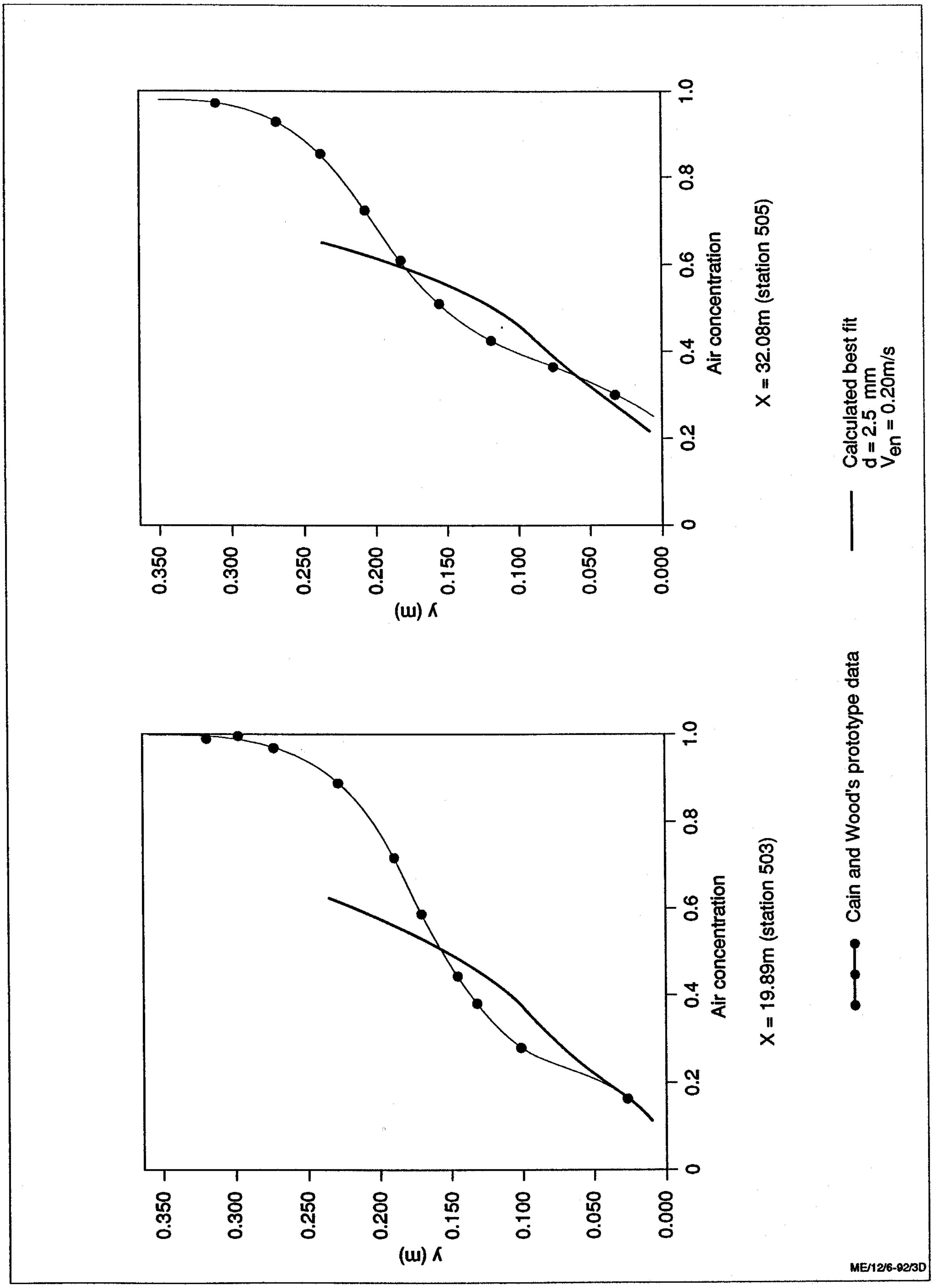

Figure 12 Comparison of calculated air concentration profiles with Cain and Wood's prototype data for Aviemore Dam spillway